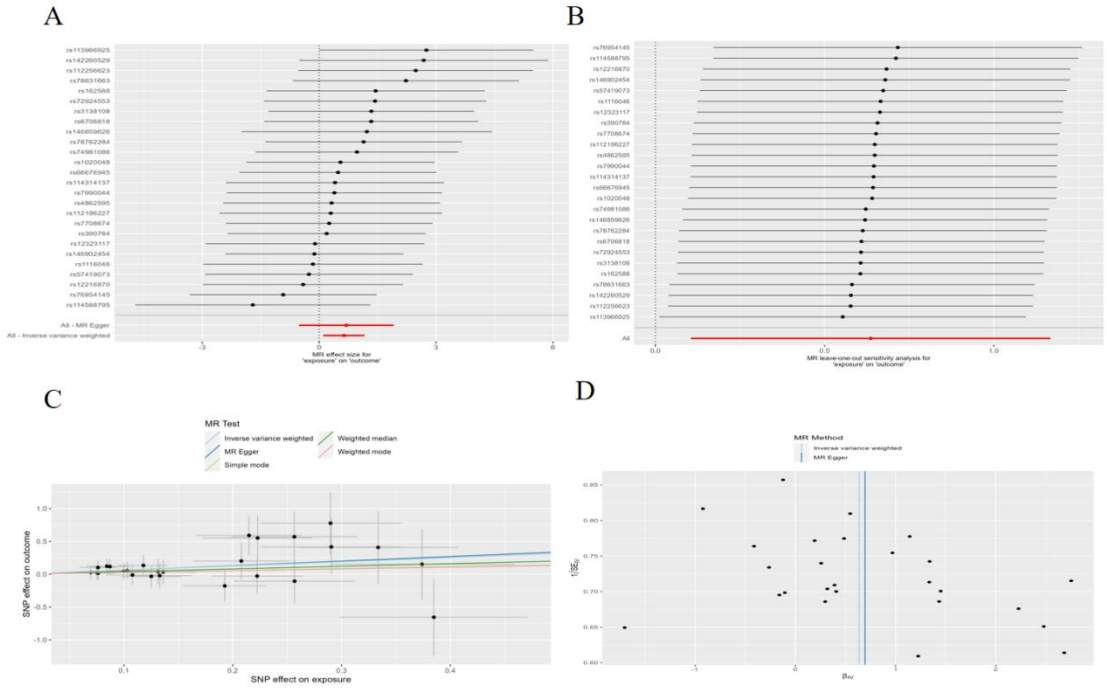

Supplementary Figure 1. Forest plot (A), sensitivity analysis (B), scatter plot (C), and funnel plot (D) of the causal effect of Methionine sulfoxide levels on PDAC risk.

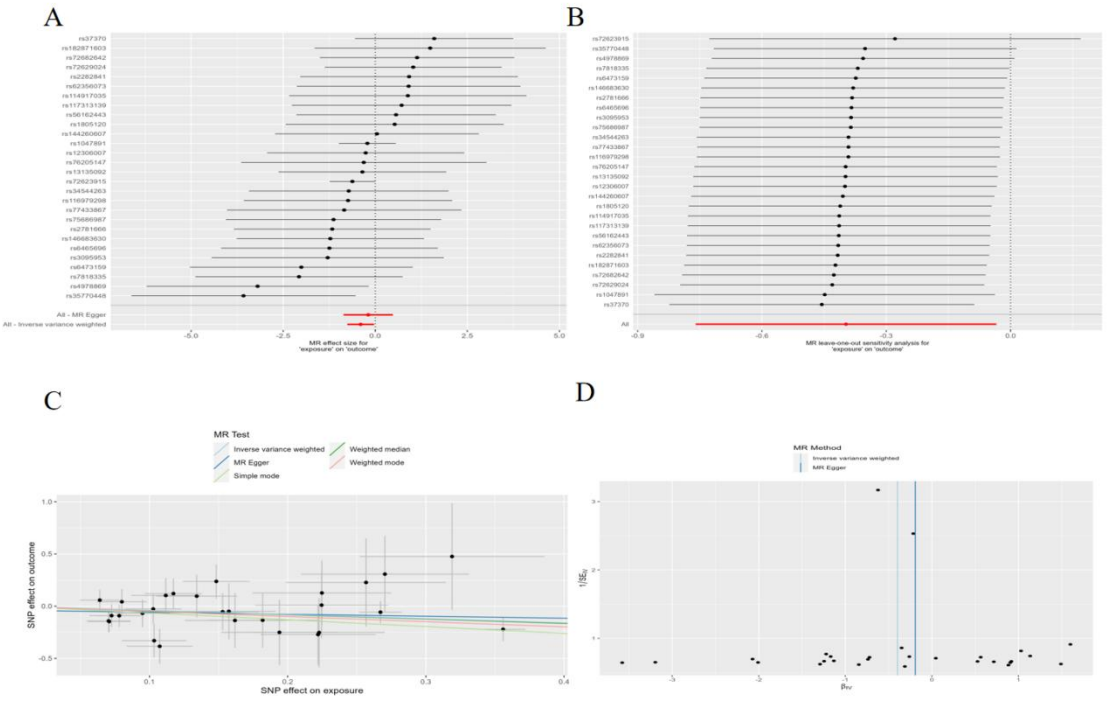

Supplementary Figure 2. Forest plot (A), sensitivity analysis (B), scatter plot (C), and funnel plot (D) of the causal effect of Homoarginine levels on PDAC risk.

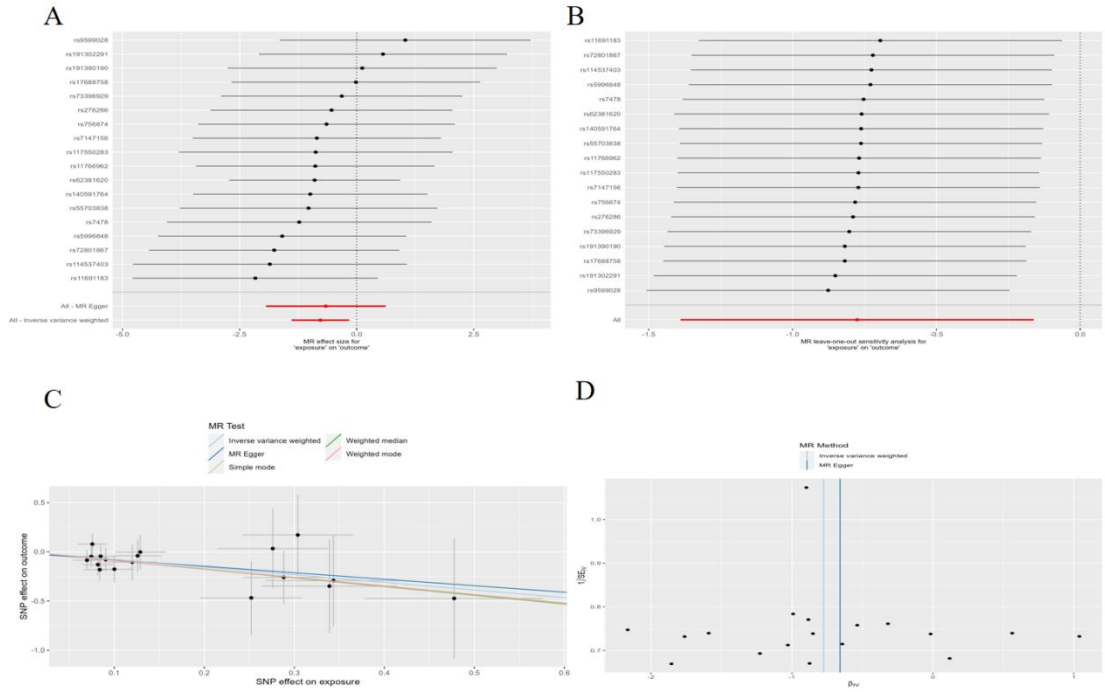

Supplementary Figure 3. Forest plot (A), sensitivity analysis (B), scatter plot (C), and funnel plot (D) of the causal effect of Tartronate (hydroxymalonate) levels on PDAC risk.

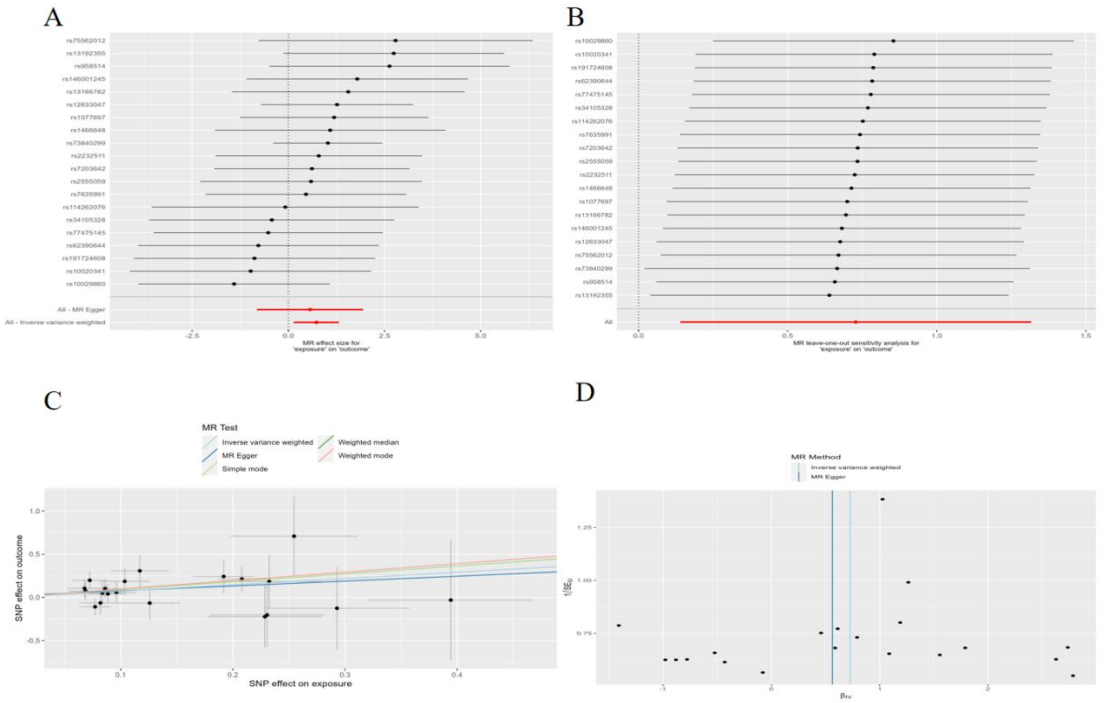

Supplementary Figure 4. Forest plot (A), sensitivity analysis (B), scatter plot (C), and funnel plot (D) of the causal effect of Erythronate levels on PDAC risk.

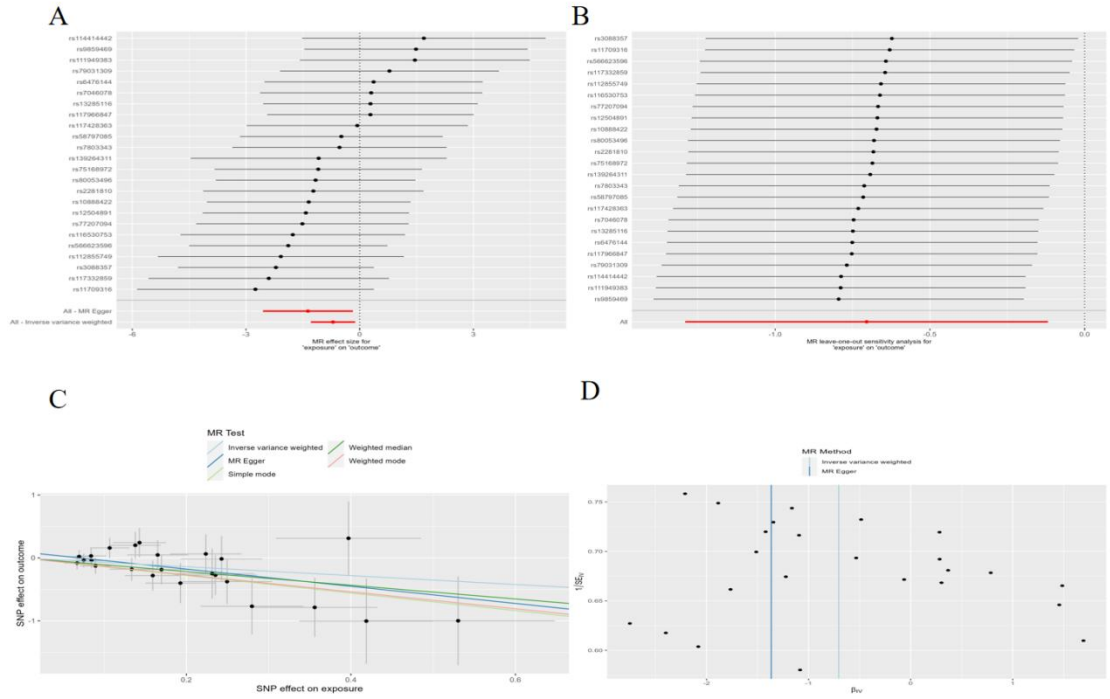

Supplementary Figure 5. Forest plot (A), scatter plot (B), and funnel plot (C) of the causal effect of Linolenate [alpha or gamma; (18:3n3 or 6)] levels on PDAC risk.

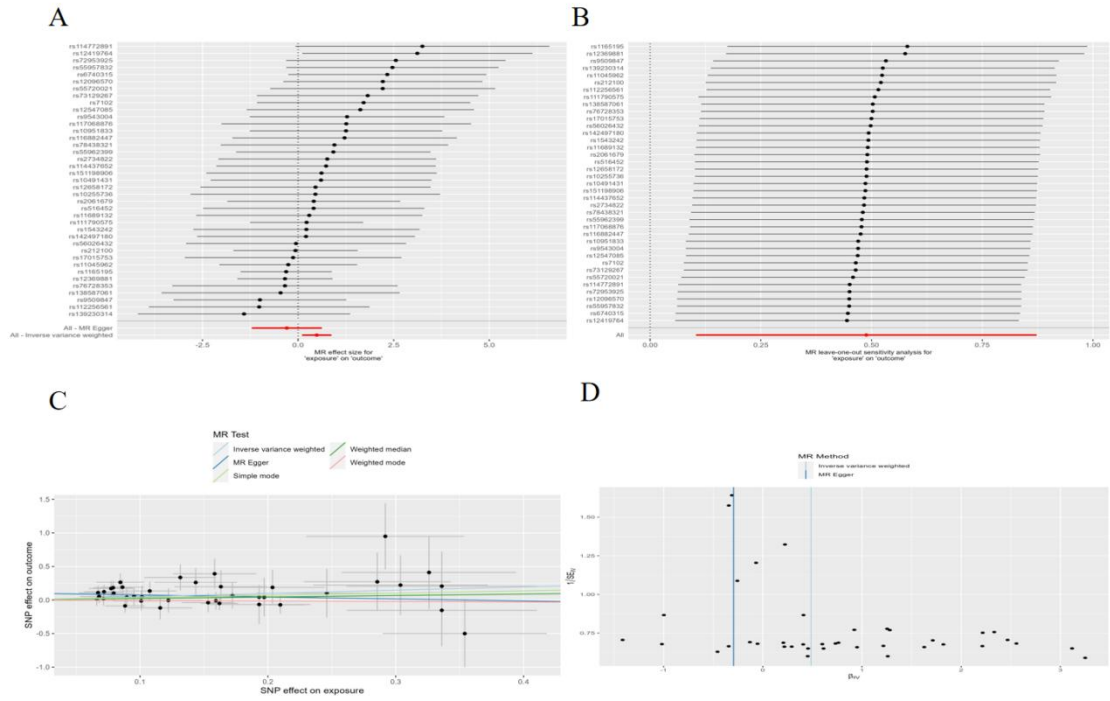

Supplementary Figure 6. Forest plot (A), sensitivity analysis (B), scatter plot (C), and funnel plot (D) of the causal effect of 21-hydroxypregnenolone disulfate levels on PDAC risk.

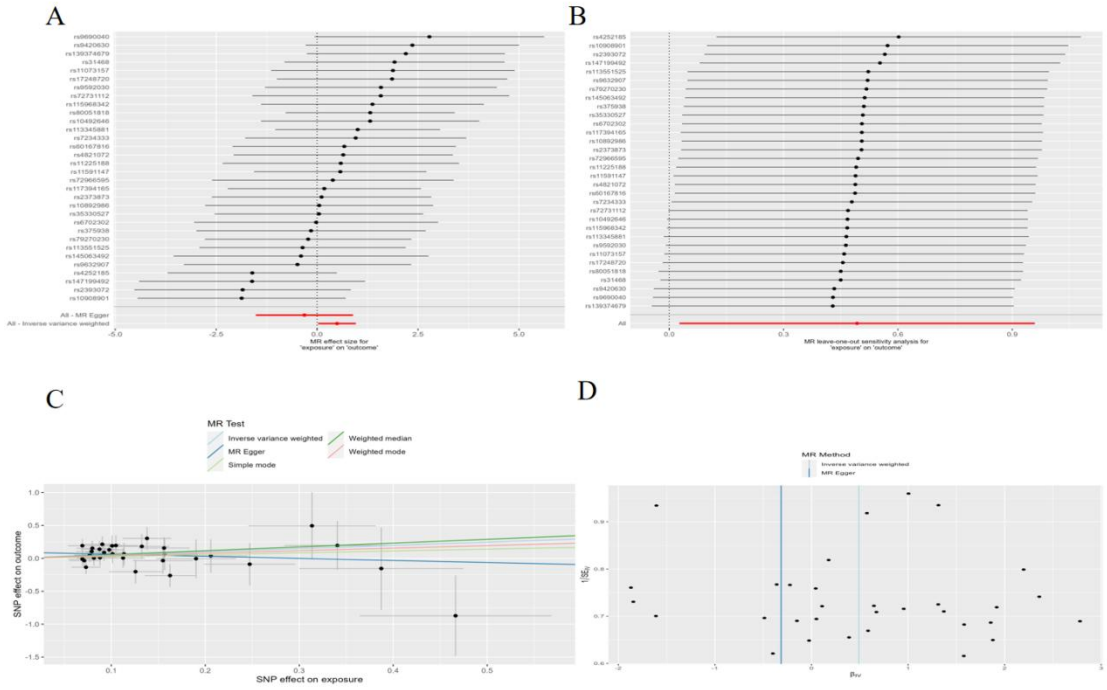

Supplementary Figure 7. Forest plot (A), sensitivity analysis (B), scatter plot (C), and funnel plot (D) of the causal effect of Palmitoyl sphingomyelin (d18:1/16:0) levels on PDAC risk.

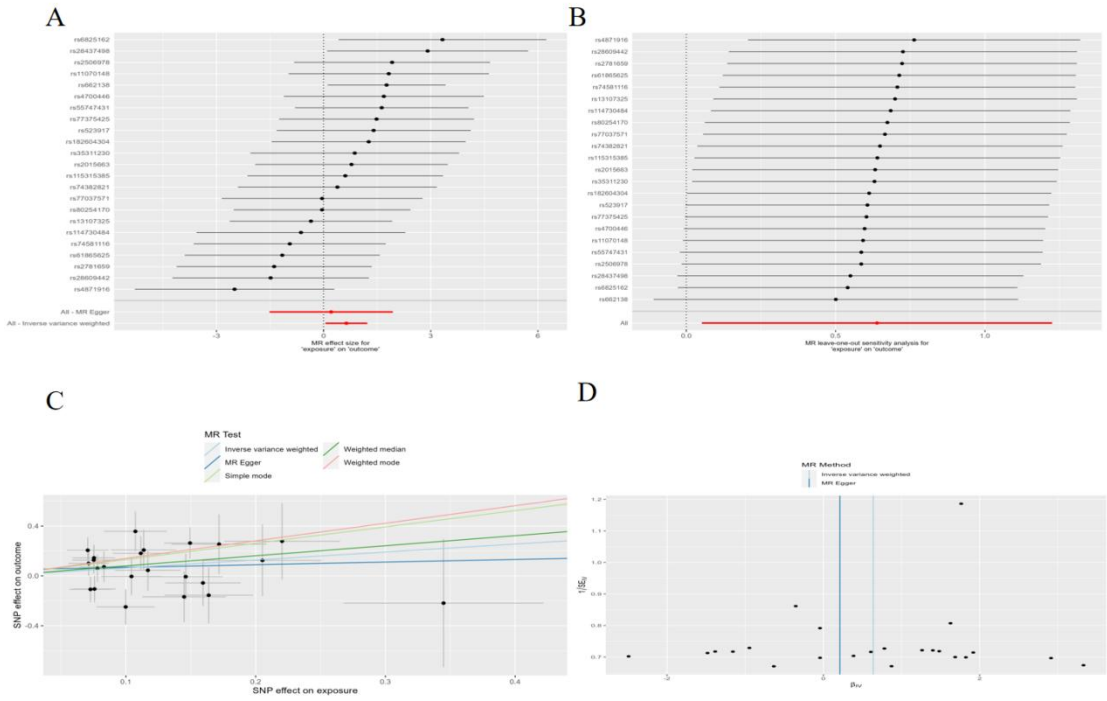

Supplementary Figure 8. Forest plot (A), sensitivity analysis (B), scatter plot (C), and funnel plot (D) of the causal effect of 2-oxoarginine levels on PDAC risk.

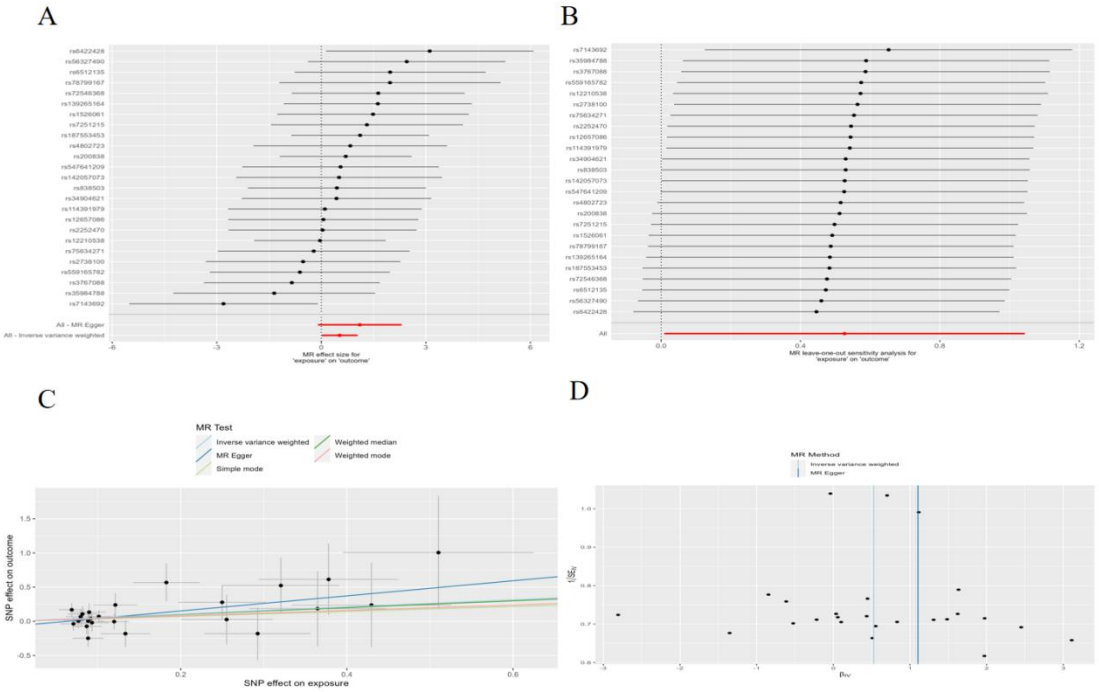

Supplementary Figure 9. Forest plot (A), sensitivity analysis (B), scatter plot (C), and funnel plot (D) of the causal effect of Margaroylcarnitine (C17) levels on PDAC risk.

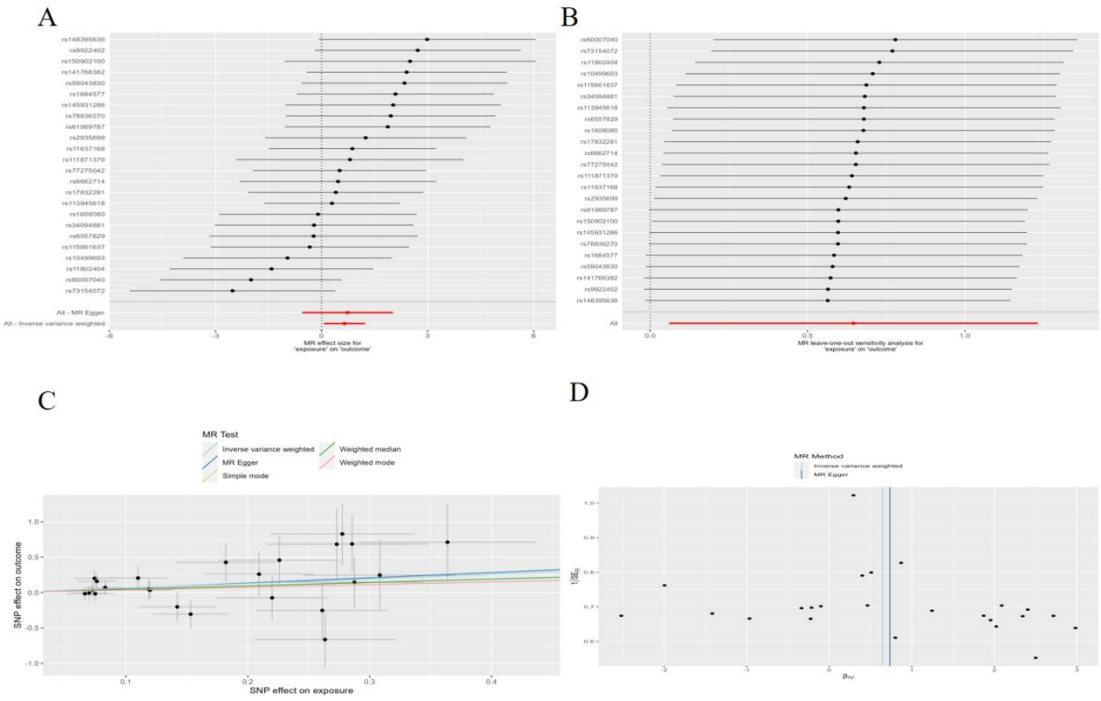

Supplementary Figure 10. Forest plot (A), sensitivity analysis (B), scatter plot (C), and funnel plot (D) of the causal effect of Vanillactate levels on PDAC risk.

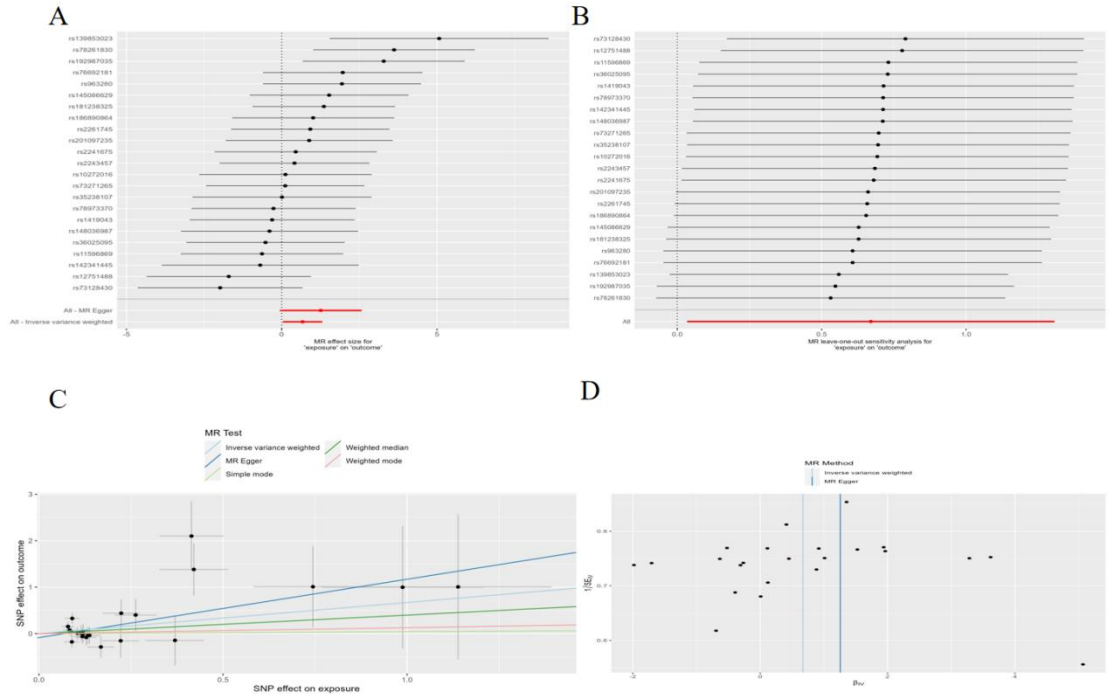

Supplementary Figure 11. Forest plot (A), sensitivity analysis (B), scatter plot (C), and funnel plot (D) of the causal effect of 1,2,3-benzenetriol sulfate (2) levels on PDAC risk.

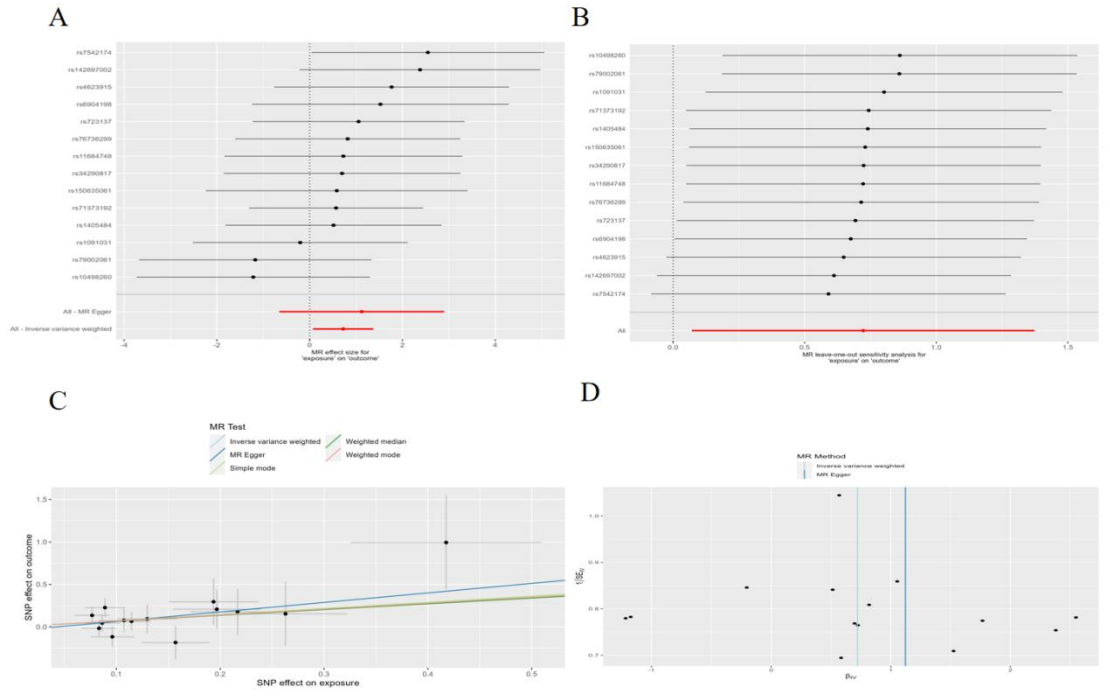

Supplementary Figure 12. Forest plot (A), sensitivity analysis (B), scatter plot (C), and funnel plot (D) of the causal effect of Trans 3,4-methyleneheptanoate levels on PDAC risk.

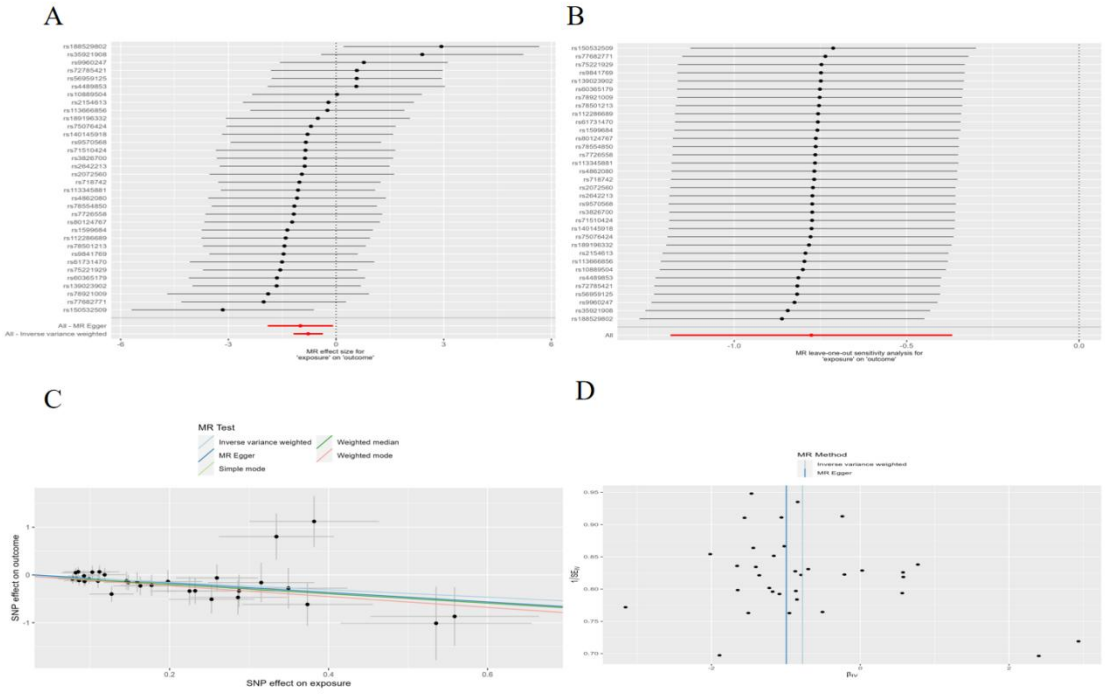

Supplementary Figure 13. Forest plot (A), sensitivity analysis (B), scatter plot (C), and funnel plot (D) of the causal effect of 1-palmitoleoylglycerol (16:1) levels on PDAC risk.

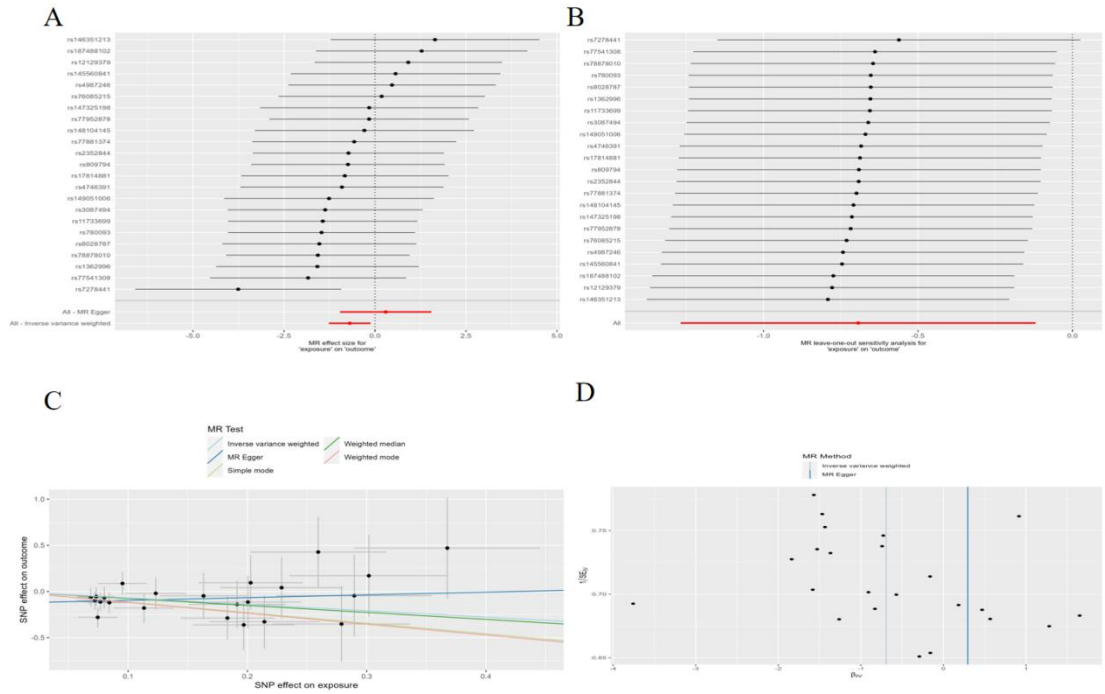

Supplementary Figure 14. Forest plot (A), sensitivity analysis (B), scatter plot (C), and funnel plot (D) of the causal effect of 1-palmitoyl-2-palmitoleoyl-gpc (16:0/16:1) levels on PDAC risk.

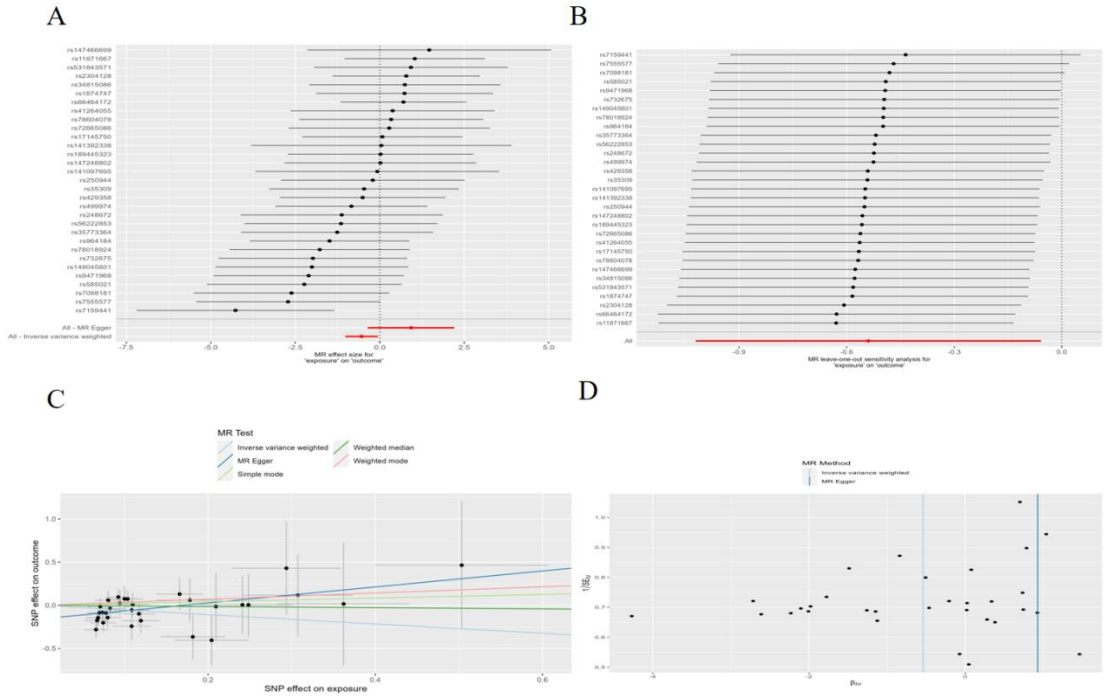

Supplementary Figure 15. Forest plot (A), sensitivity analysis (B), scatter plot (C), and funnel plot (D) of the causal effect of 1-oleoyl-2-docosahexaenoyl-GPC (18:1/22:6) levels on PDAC risk.

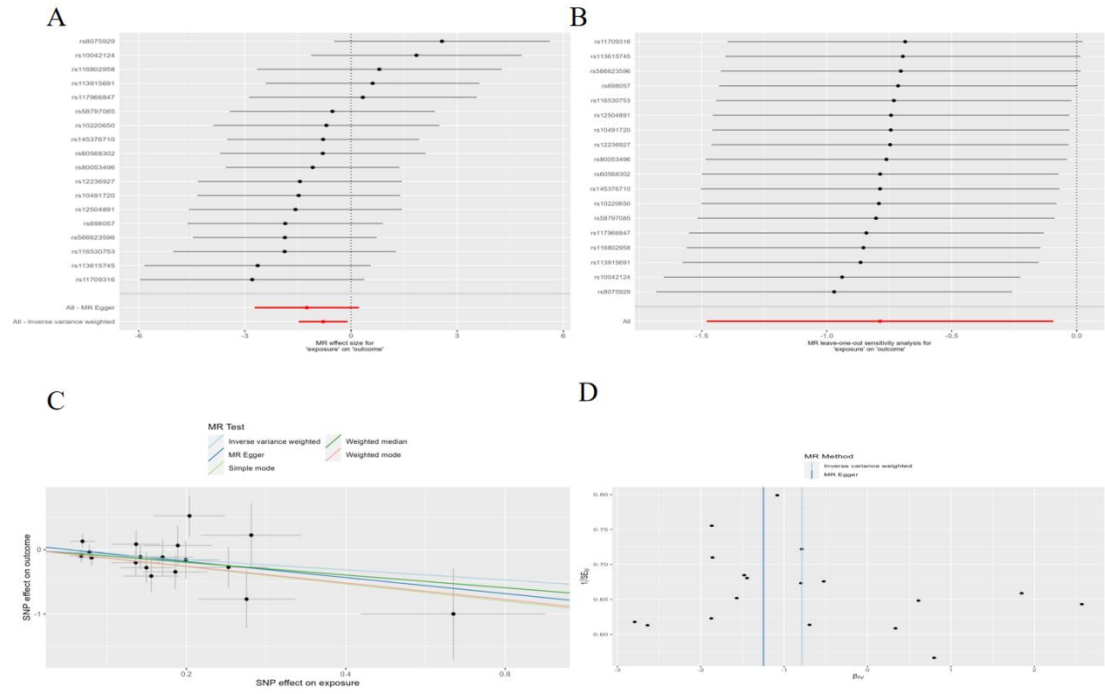

Supplementary Figure 16. Forest plot (A), sensitivity analysis (B), scatter plot (C), and funnel plot (D) of the causal effect of Hexadecadienoate (16:2n6) levels on PDAC risk.

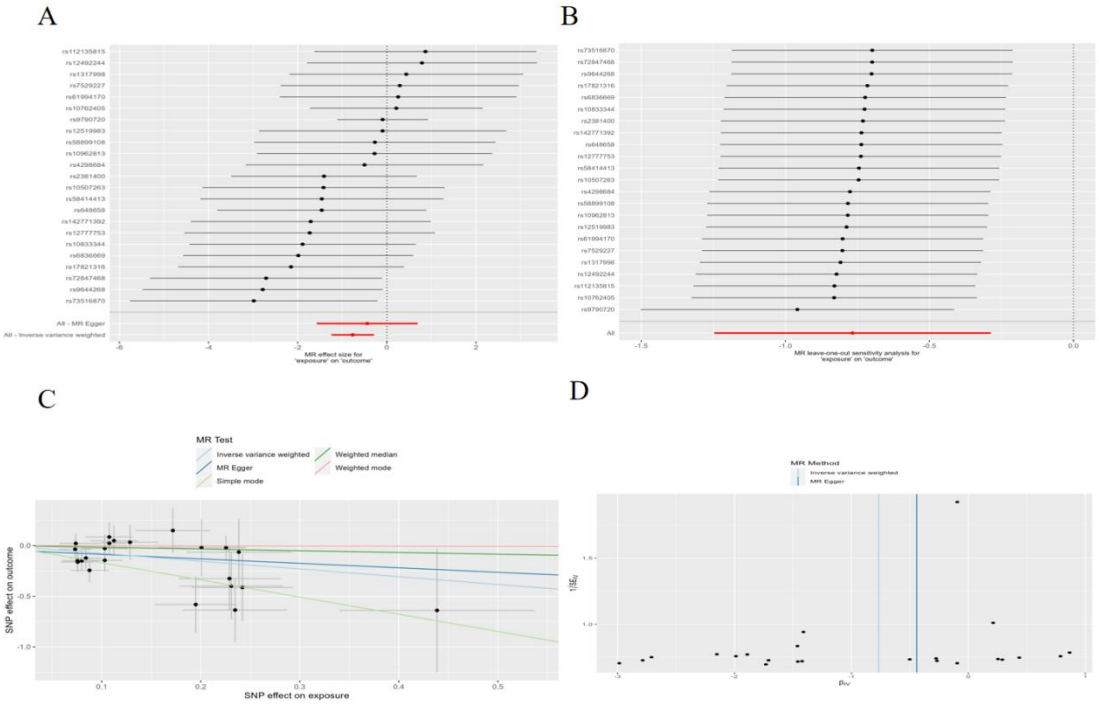

Supplementary Figure 17. Forest plot (A), sensitivity analysis (B), scatter plot (C), and funnel plot (D) of the causal effect of Glycosyl-N-tricosanoyl-sphingadienine (d18:2/23:0) levels on PDAC risk.

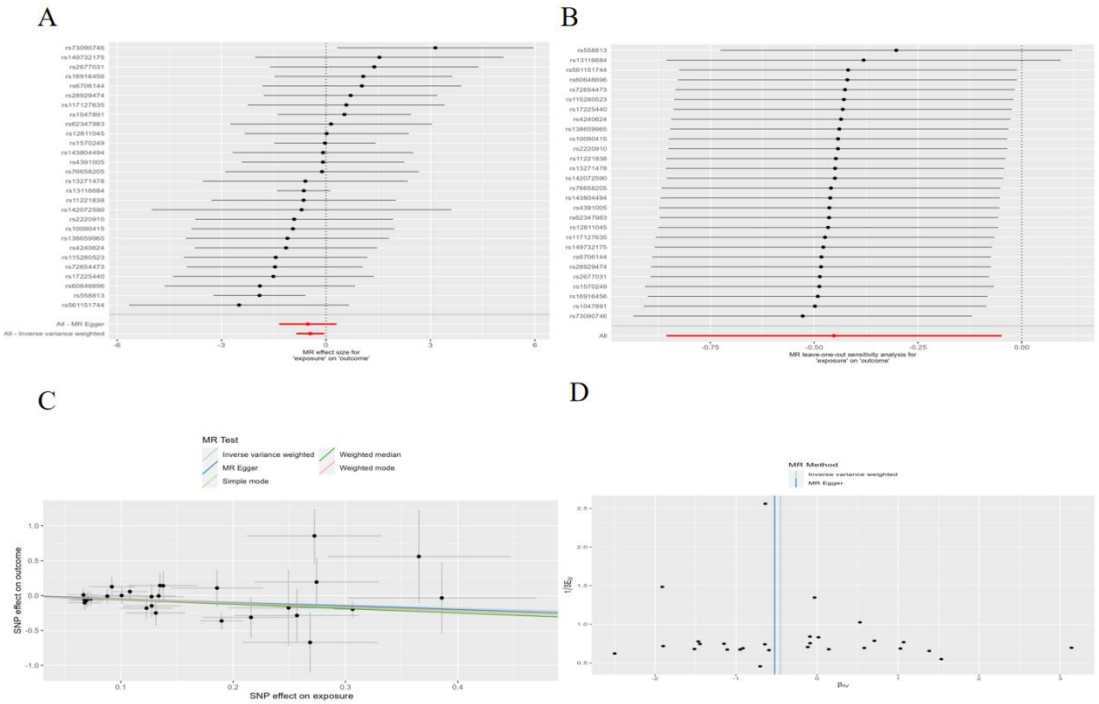

Supplementary Figure 18. Forest plot (A), sensitivity analysis (B), scatter plot (C), and funnel plot (D) of the causal effect of Glycosyl-N-(2-hydroxynervonoyl)-sphingosine (d18:1/24:1(2OH)) levels on

PDAC risk.

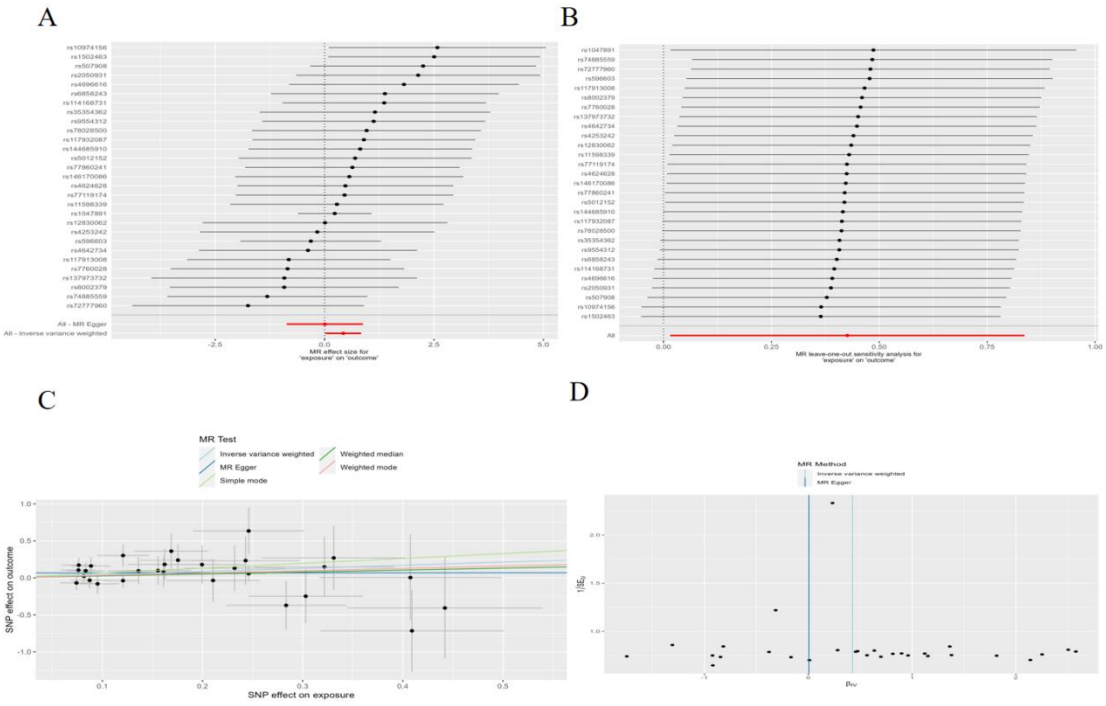

Supplementary Figure 19. Forest plot (A), sensitivity analysis (B), scatter plot (C), and funnel plot (D) of the causal effect of Trans-2-hexenoylglycine levels on PDAC risk.

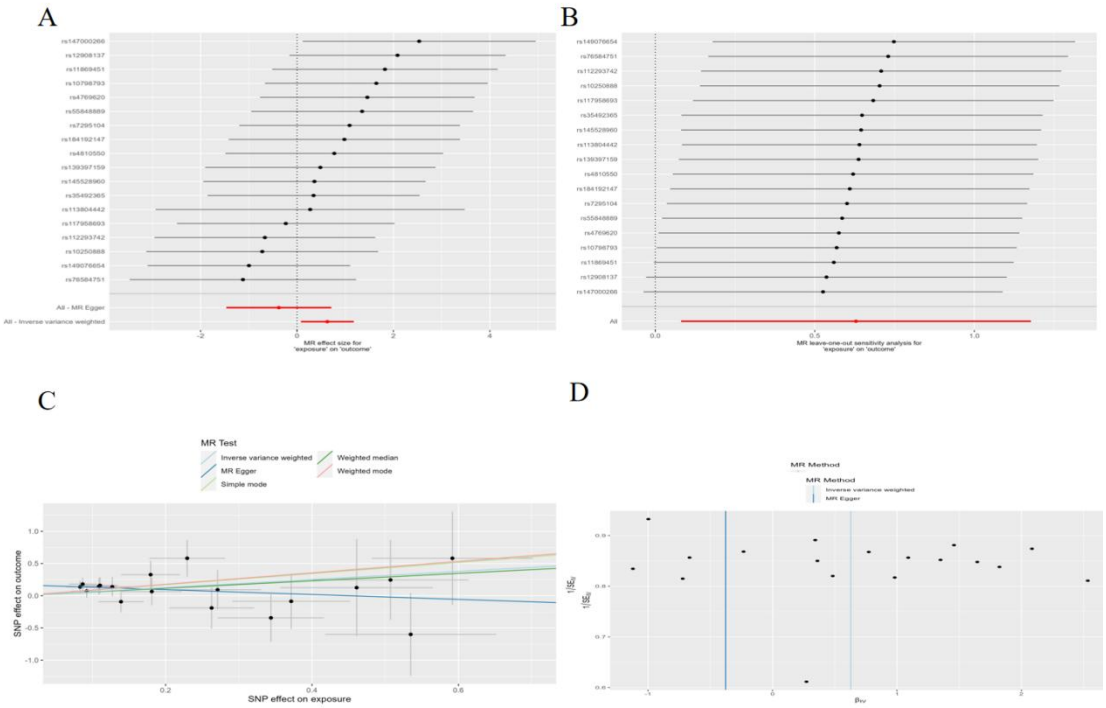

Supplementary Figure 20. Forest plot (A), sensitivity analysis (B), scatter plot (C), and funnel plot (D) of the causal effect of 3-hydroxyphenylacetoylglutamine levels on PDAC risk.

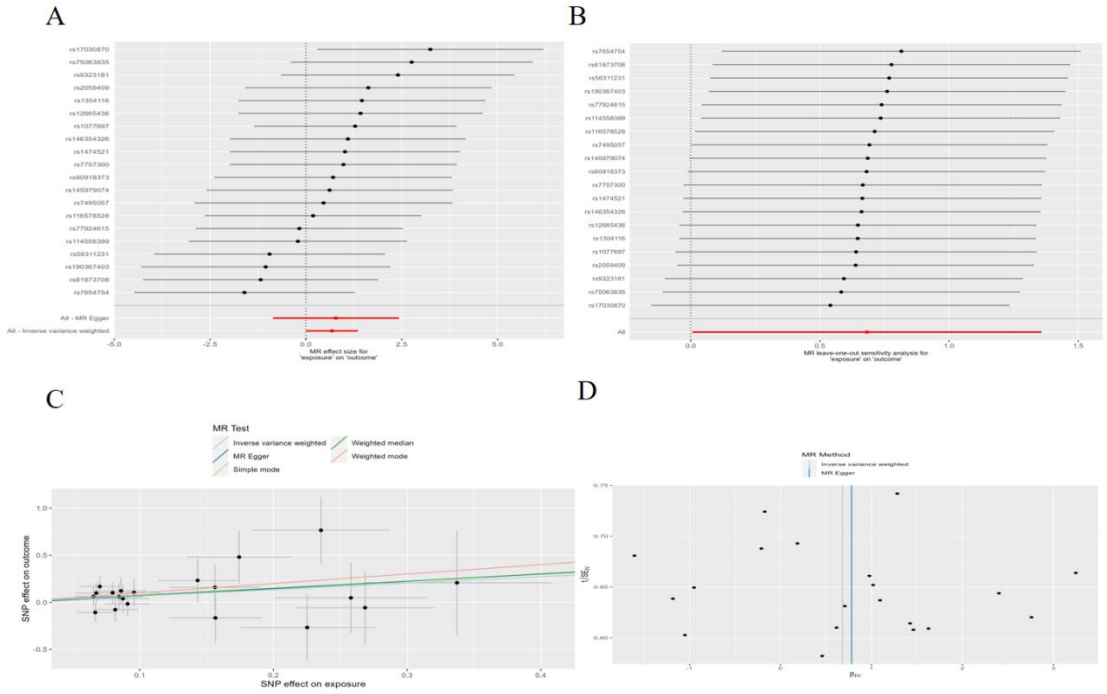

Supplementary Figure 21. Forest plot (A), sensitivity analysis (B), scatter plot (C), and funnel plot (D) of the causal effect of Hydroxyasparagine levels on PDAC risk.

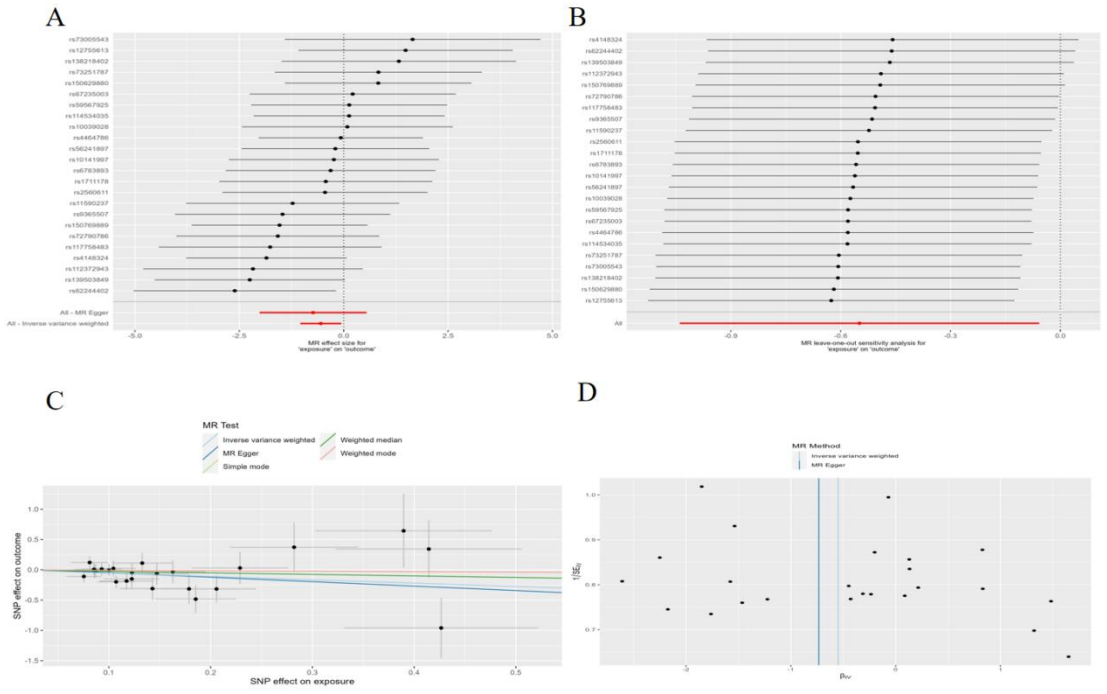

Supplementary Figure 22. Forest plot (A), sensitivity analysis (B), scatter plot (C), and funnel plot (D) of the causal effect of 8-methoxykynurenate levels on PDAC risk.

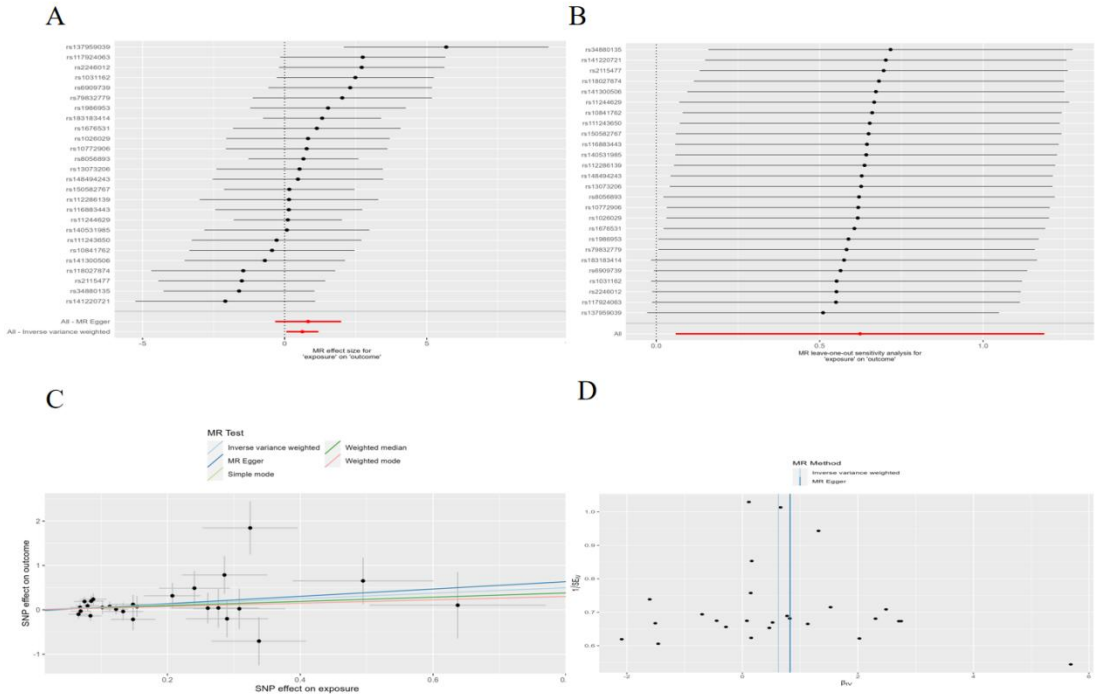

Supplementary Figure 23. Forest plot (A), sensitivity analysis (B), scatter plot (C), and funnel plot (D) of the causal effect of 3-amino-2-piperidone levels on PDAC risk.

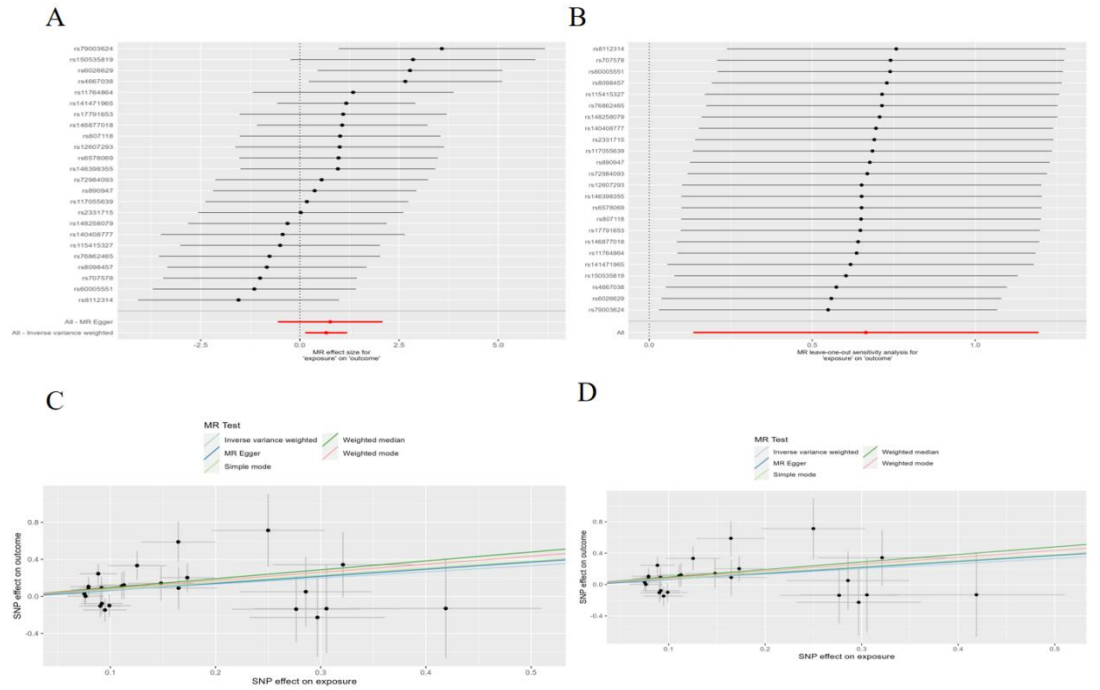

Supplementary Figure 24. Forest plot (A), sensitivity analysis (B), scatter plot (C), and funnel plot (D) of the causal effect of Sulfate of piperine metabolite C18H21NO3 (1) levels on PDAC risk.

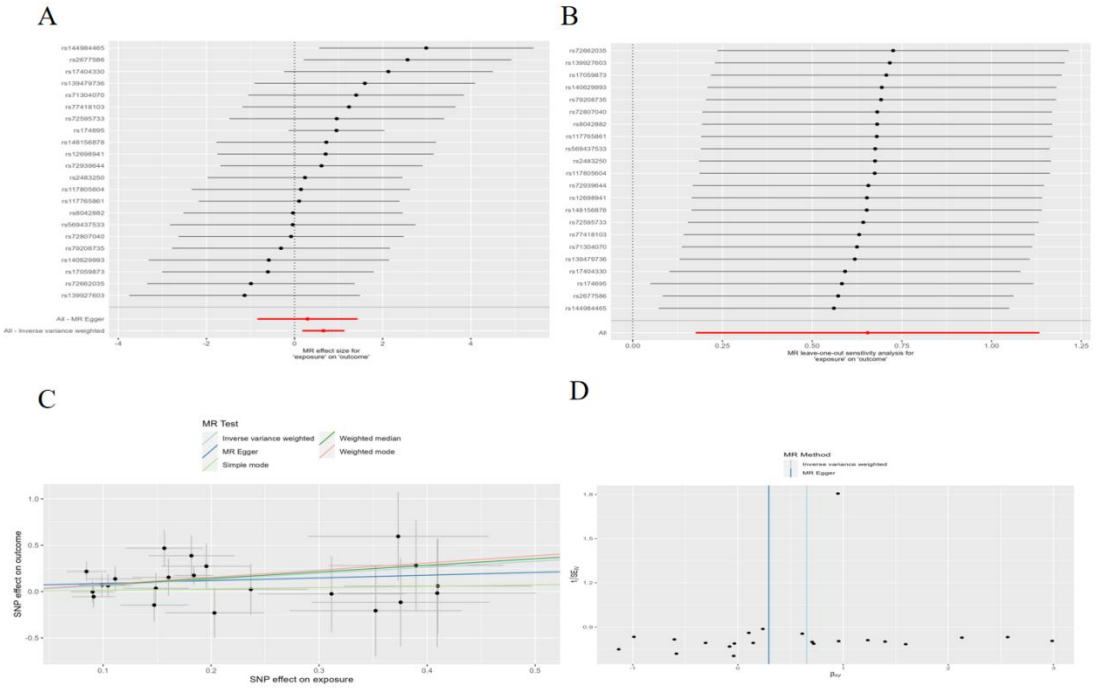

Supplementary Figure 25. Forest plot (A), sensitivity analysis (B), scatter plot (C), and funnel plot (D) of the causal effect of Glucuronide of piperine metabolite C17H21NO3 (5) levels on PDAC risk.

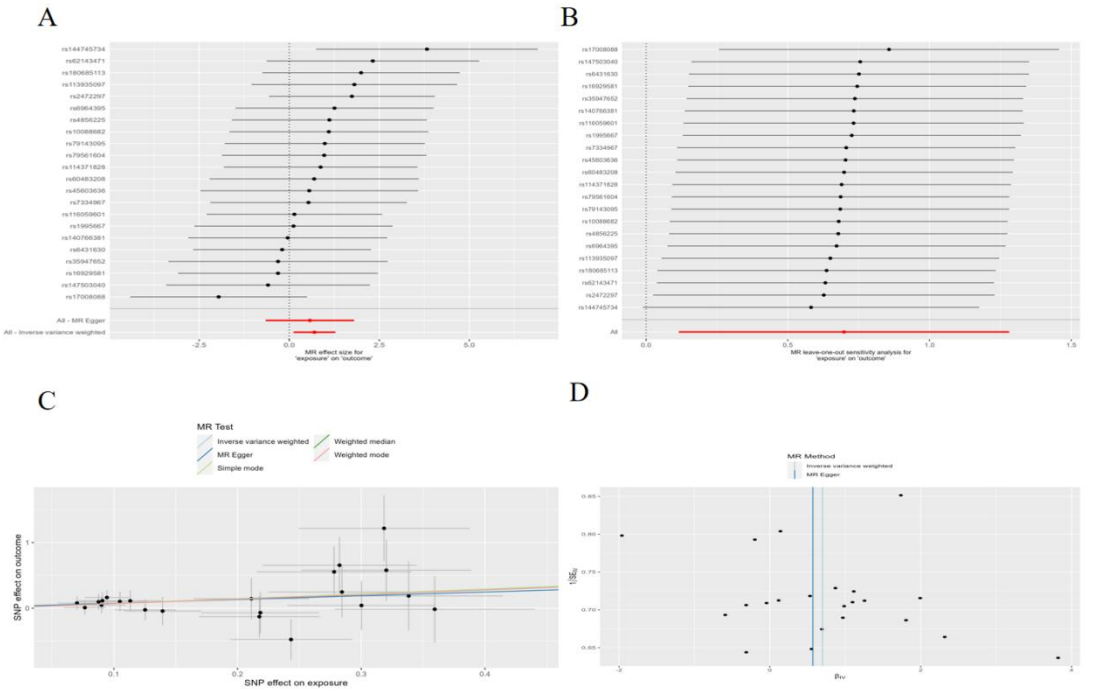

Supplementary Figure 26. Forest plot (A), sensitivity analysis (B), scatter plot (C), and funnel plot (D) of the causal effect of 4-ethylcatechol sulfate levels on PDAC risk.

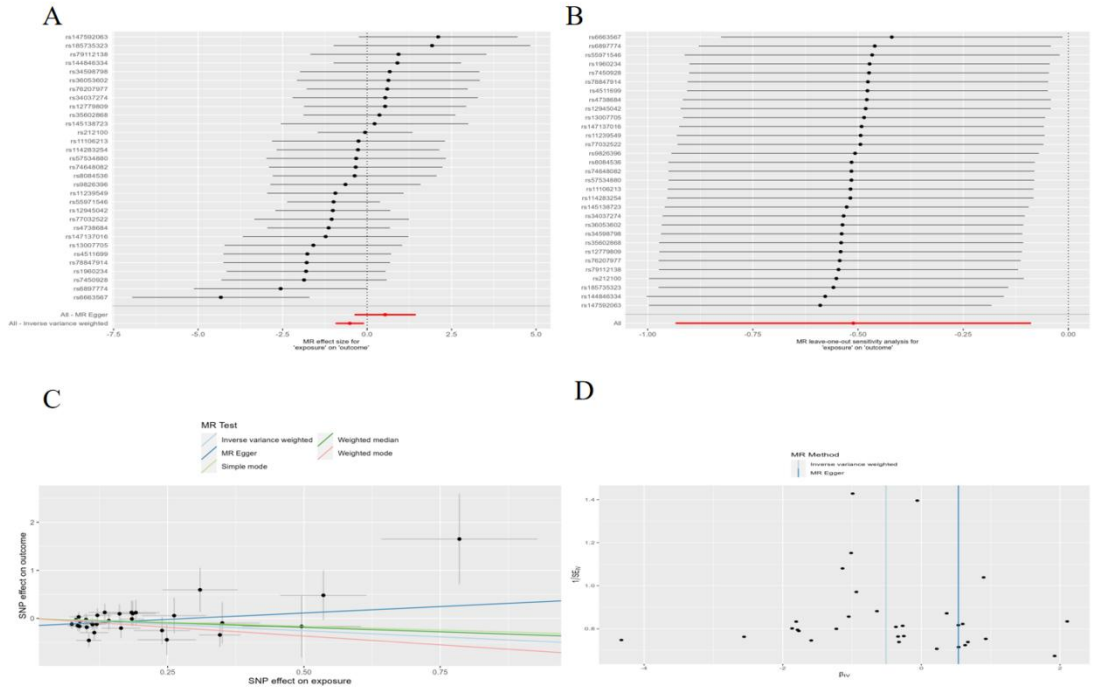

Supplementary Figure 27. Forest plot (A), sensitivity analysis (B), scatter plot (C), and funnel plot (D) of the causal effect of Taurochenodeoxycholic acid 3-sulfate levels on PDAC risk.

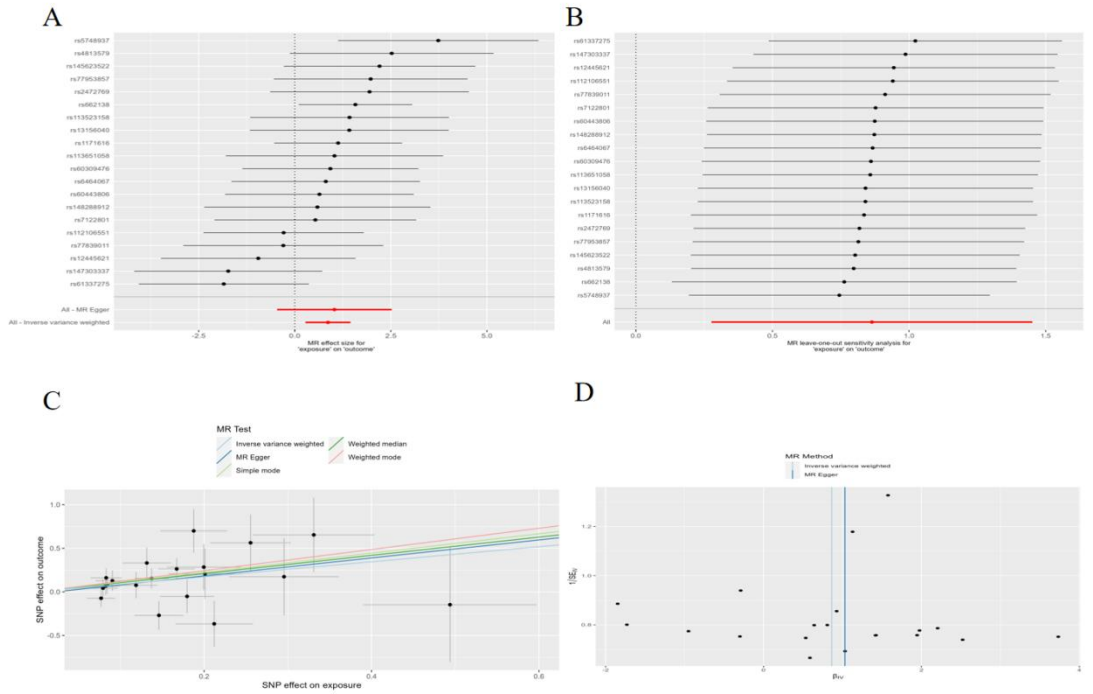

Supplementary Figure 28. Forest plot (A), sensitivity analysis (B), scatter plot (C), and funnel plot (D) of the causal effect of Levulinoylcarnitine levels on PDAC risk.

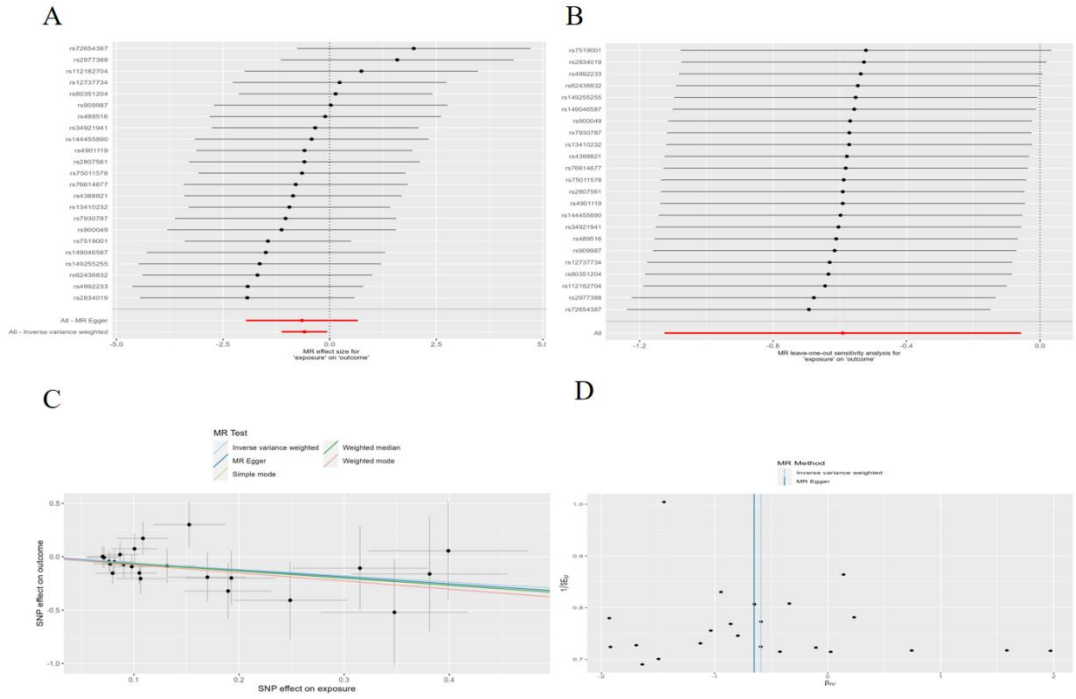

Supplementary Figure 29. Forest plot (A), sensitivity analysis (B), scatter plot (C), and funnel plot (D) of the causal effect of S-carboxyethylcysteine levels on PDAC risk.

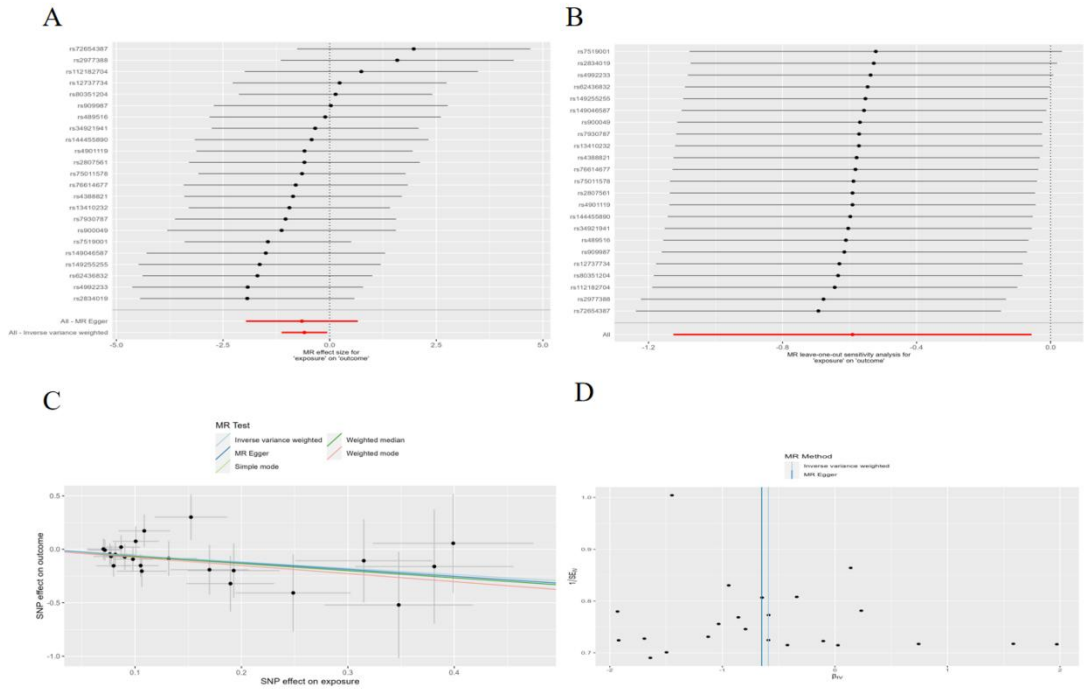

Supplementary Figure 30. Forest plot (A), sensitivity analysis (B), scatter plot (C), and funnel plot (D) of the causal effect of Bilirubin degradation product, C17H20N2O5 (2) levels on PDAC risk.

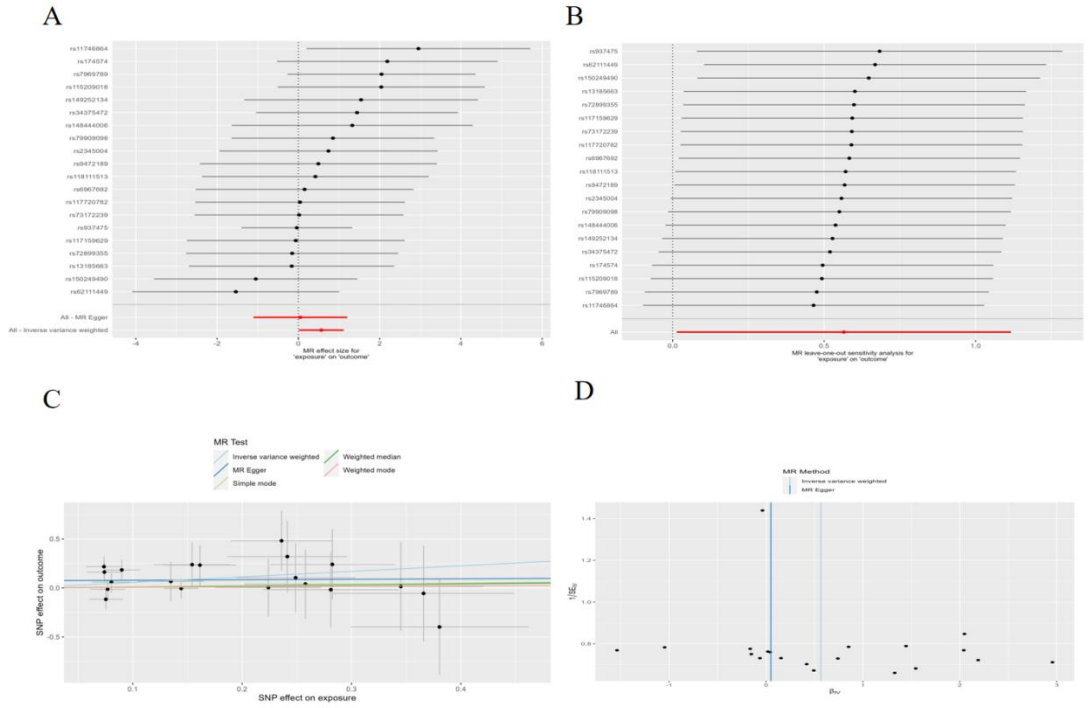

Supplementary Figure 31. Forest plot (A), sensitivity analysis (B), scatter plot (C), and funnel plot (D) of the causal effect of Phenylalanine levels on PDAC risk.

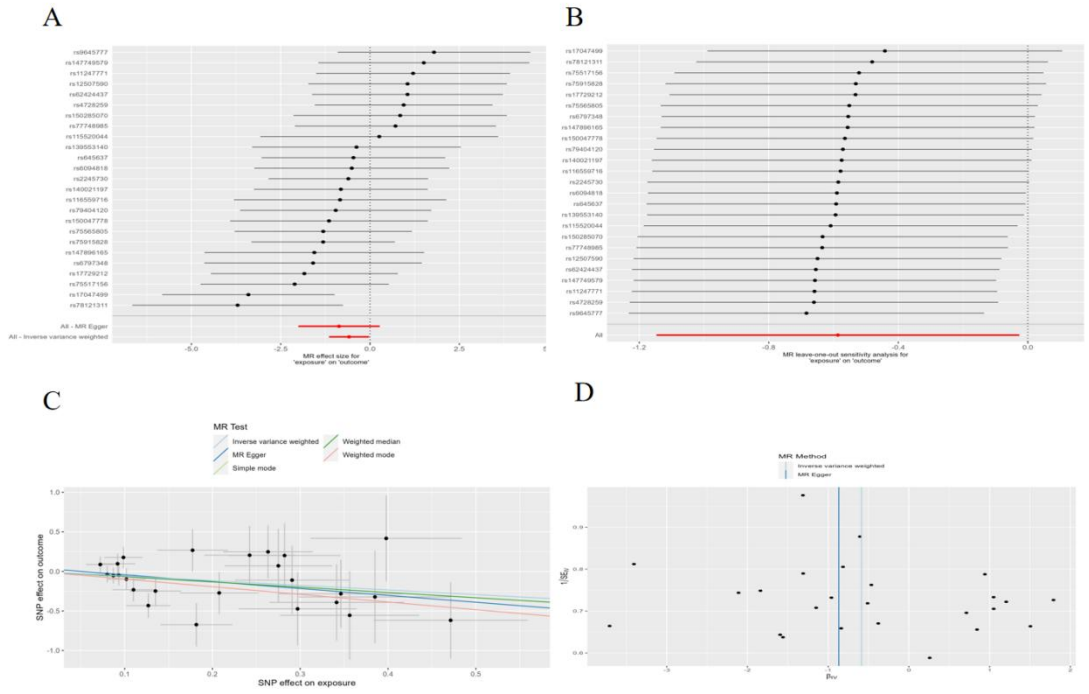

Supplementary Figure 32. Forest plot (A), sensitivity analysis (B), scatter plot (C), and funnel plot (D) of the causal effect of Caffeine levels on PDAC risk.

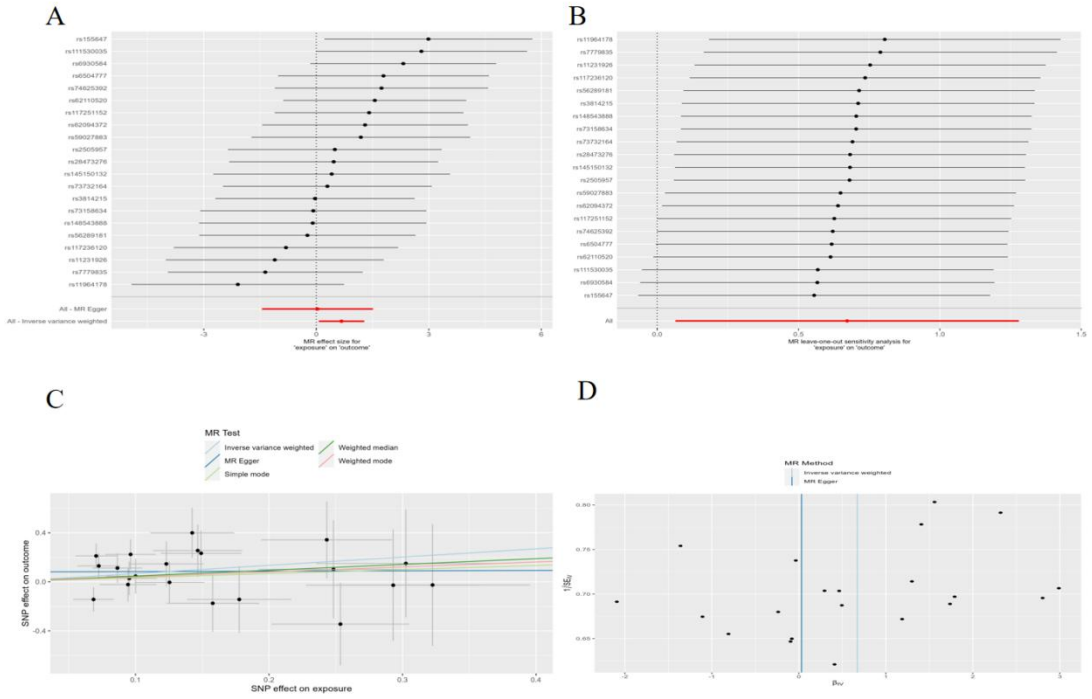

Supplementary Figure 33. Forest plot (A), sensitivity analysis (B), scatter plot (C), and funnel plot (D) of the causal effect of Valine levels on PDAC risk.

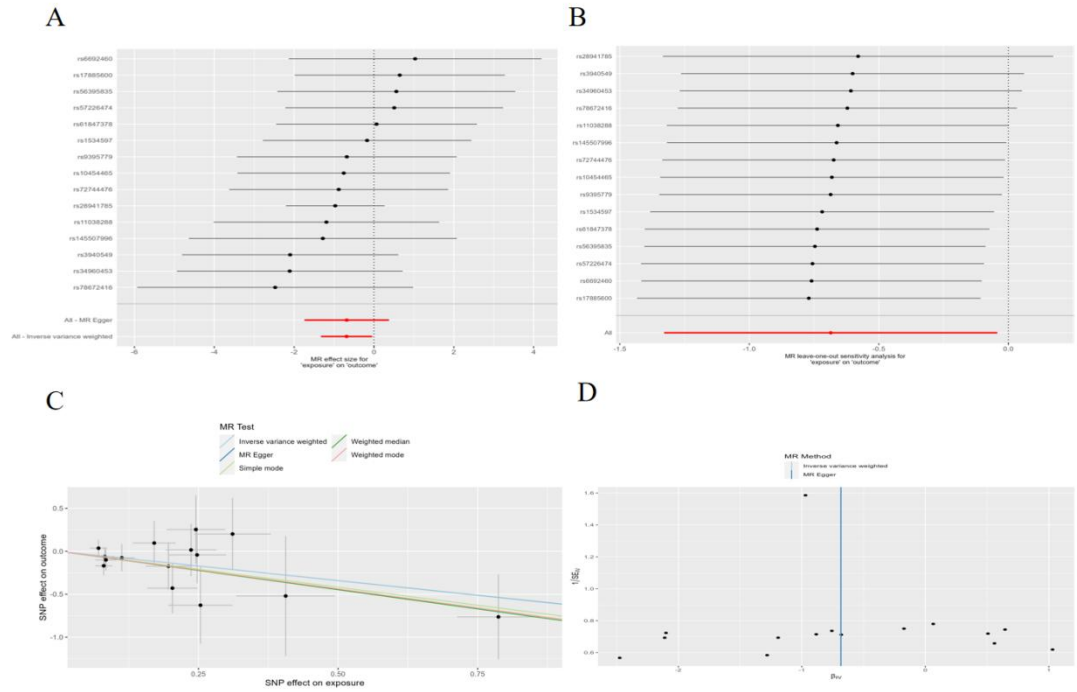

Supplementary Figure 34. Forest plot (A), sensitivity analysis (B), scatter plot (C), and funnel plot (D) of the causal effect of X-11795 levels on PDAC risk.

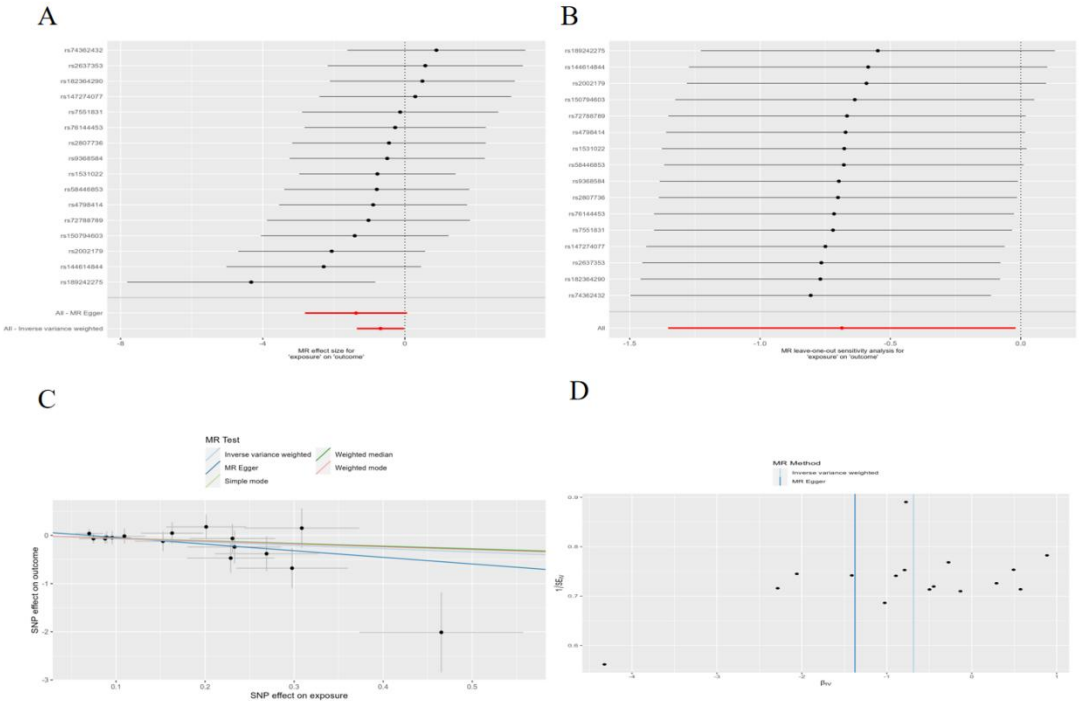

Supplementary Figure 35. Forest plot (A), sensitivity analysis (B), scatter plot (C), and funnel plot (D) of the causal effect of X-12007 levels on PDAC risk.

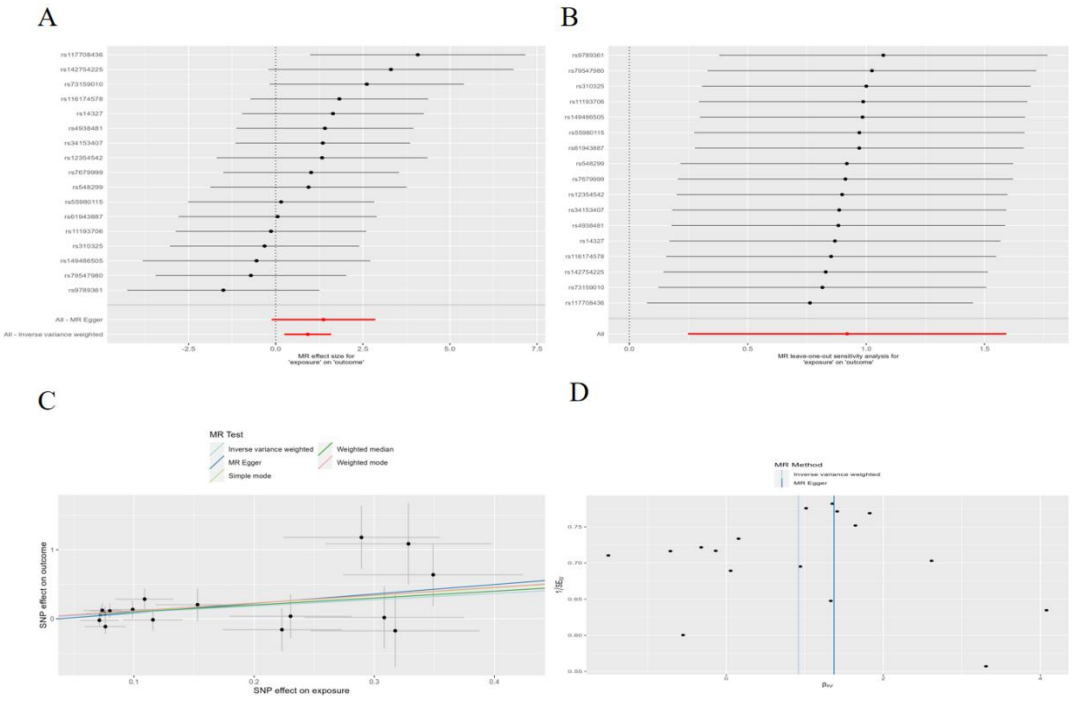

Supplementary Figure 36. Forest plot (A), sensitivity analysis (B), scatter plot (C), and funnel plot (D) of the causal effect of X-12906 levels on PDAC risk.

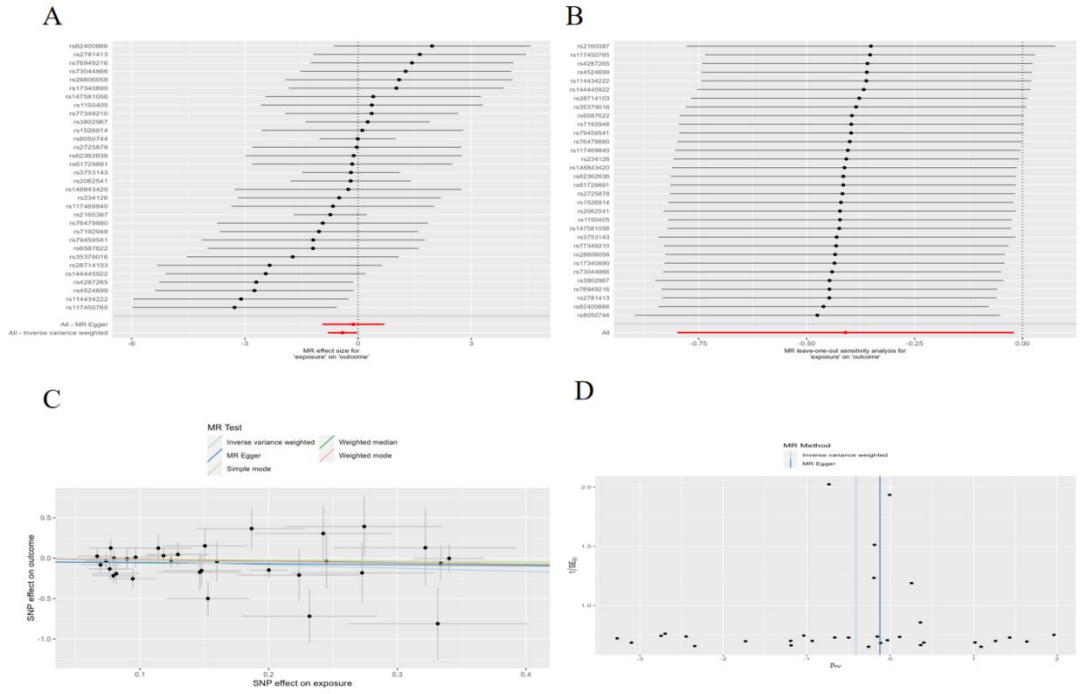

Supplementary Figure 37. Forest plot (A), sensitivity analysis (B), scatter plot (C), and funnel plot (D) of the causal effect of X-13684 levels on PDAC risk.

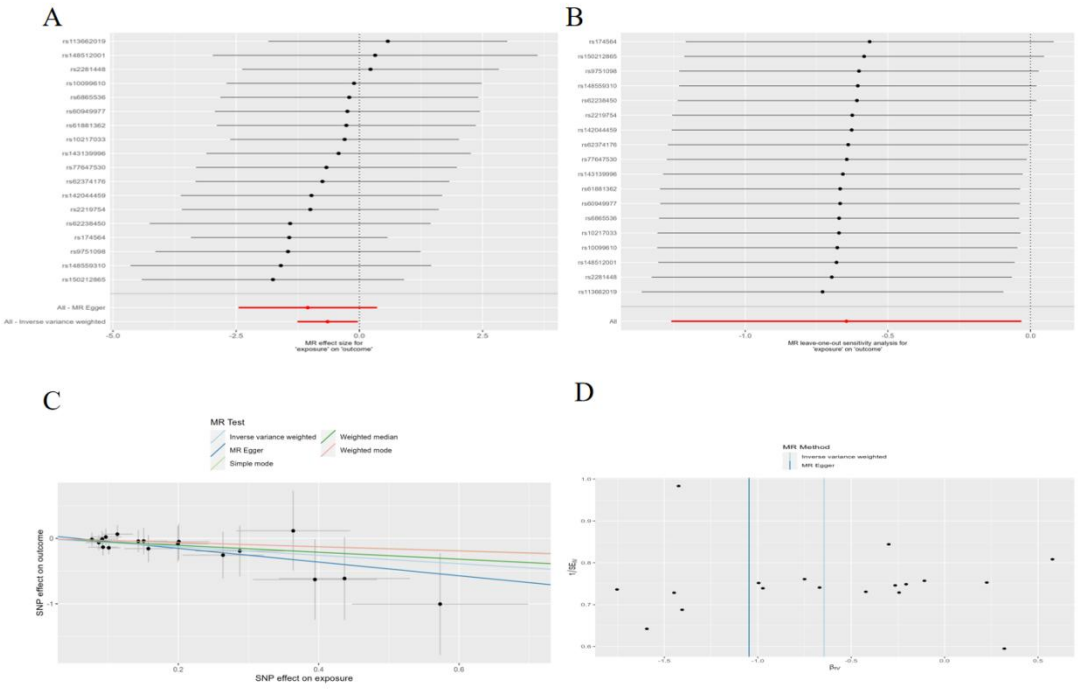

Supplementary Figure 38. Forest plot (A), sensitivity analysis (B), scatter plot (C), and funnel plot (D) of the causal effect of X-17010 levels on PDAC risk.

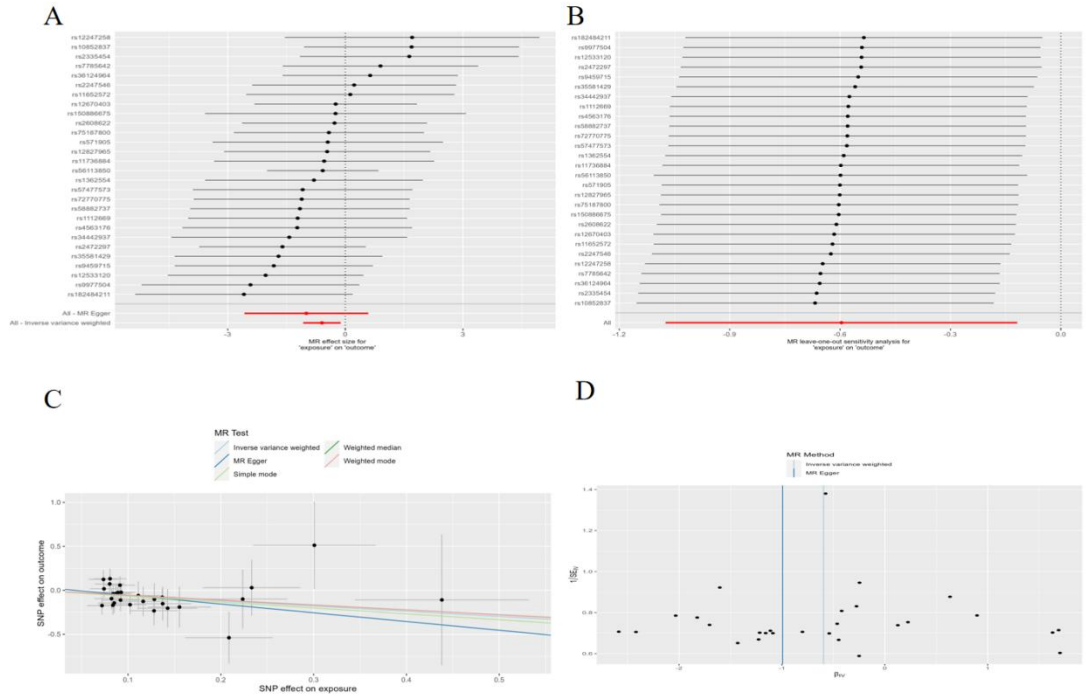

Supplementary Figure 39. Forest plot (A), sensitivity analysis (B), scatter plot (C), and funnel plot (D) of the causal effect of X-21286 levels on PDAC risk.

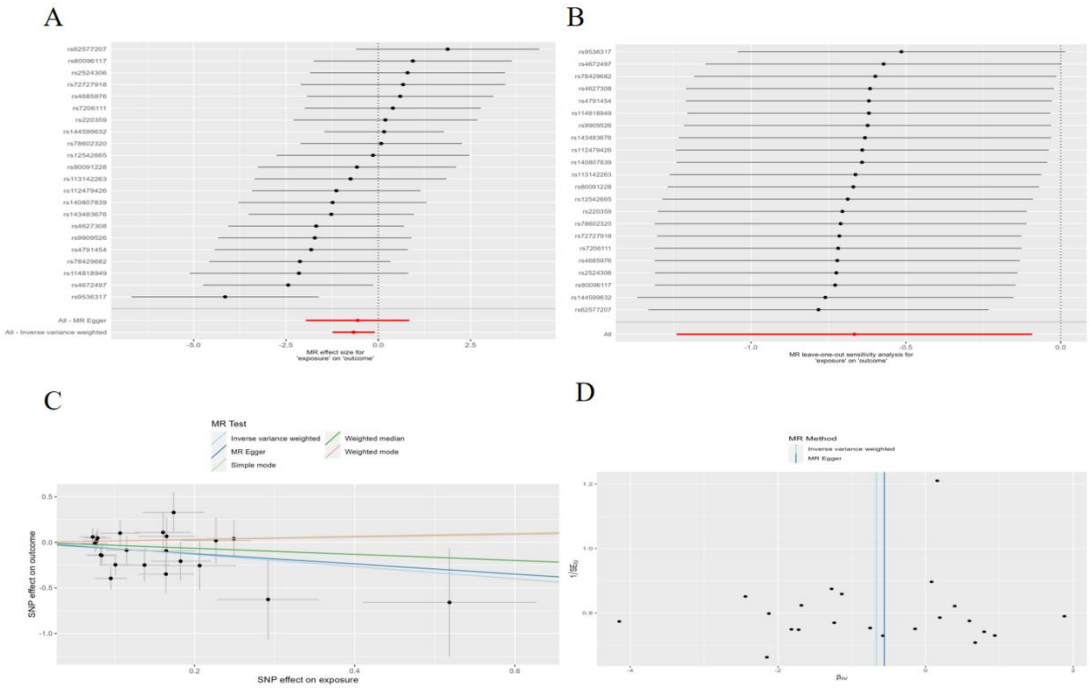

Supplementary Figure 40. Forest plot (A), sensitivity analysis (B), scatter plot (C), and funnel plot (D) of the causal effect of X-21834 levels on PDAC risk.

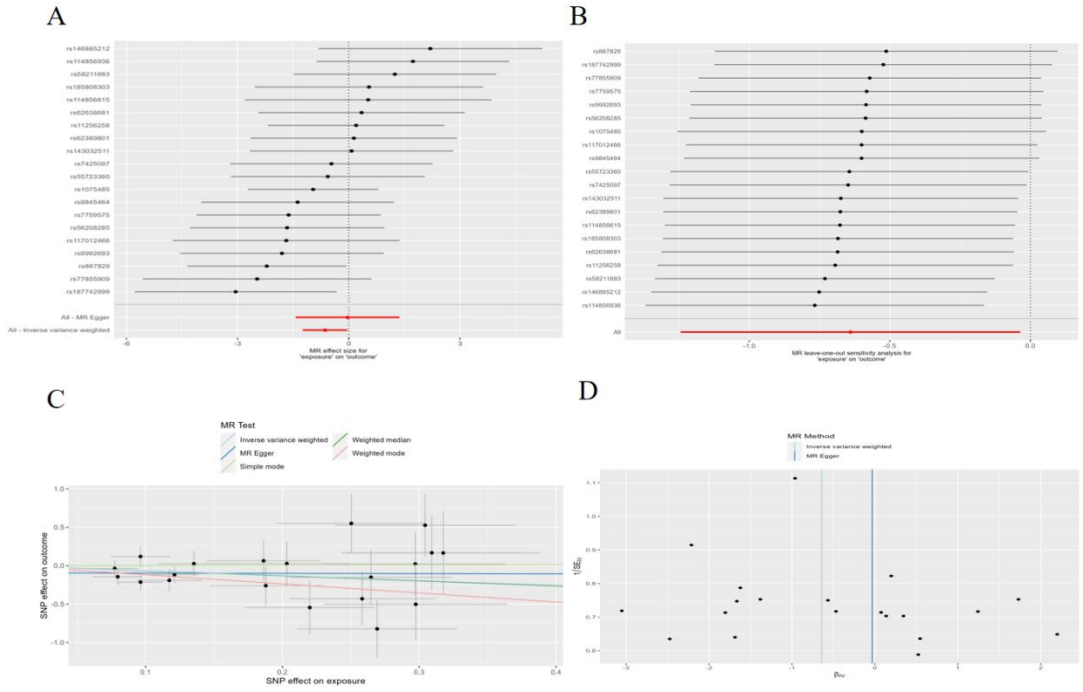

Supplementary Figure 41. Forest plot (A), sensitivity analysis (B), scatter plot (C), and funnel plot (D) of the causal effect of X-23974 levels on PDAC risk.

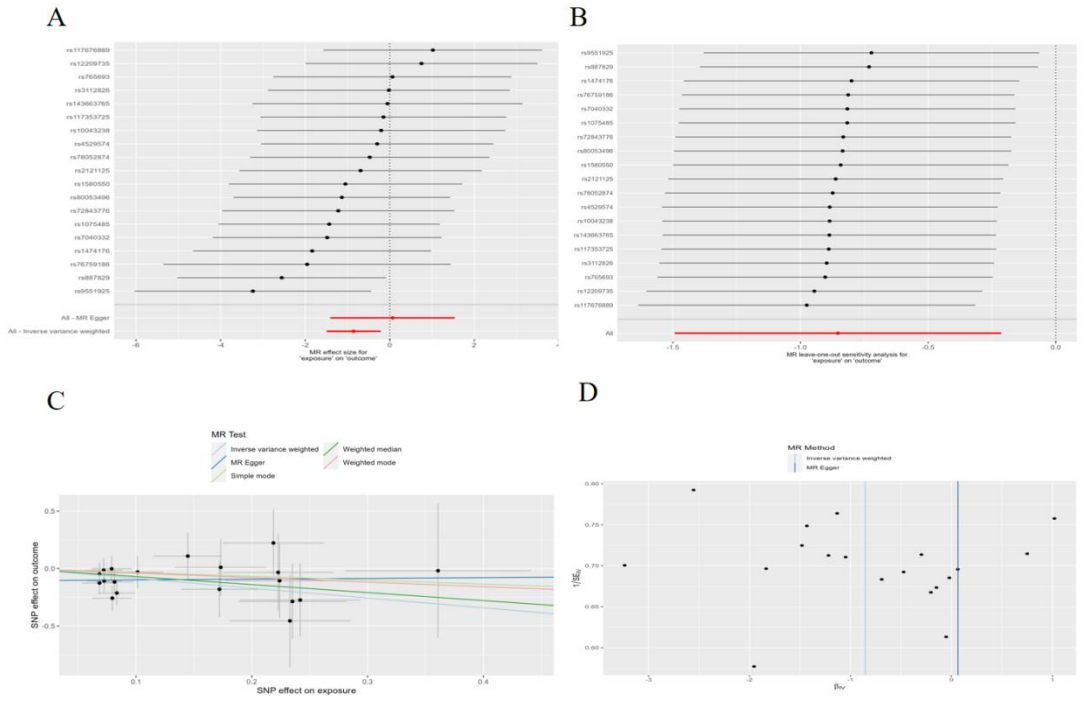

Supplementary Figure 42. Forest plot (A), sensitivity analysis (B), scatter plot (C), and funnel plot (D) of the causal effect of X-23782 levels on PDAC risk.

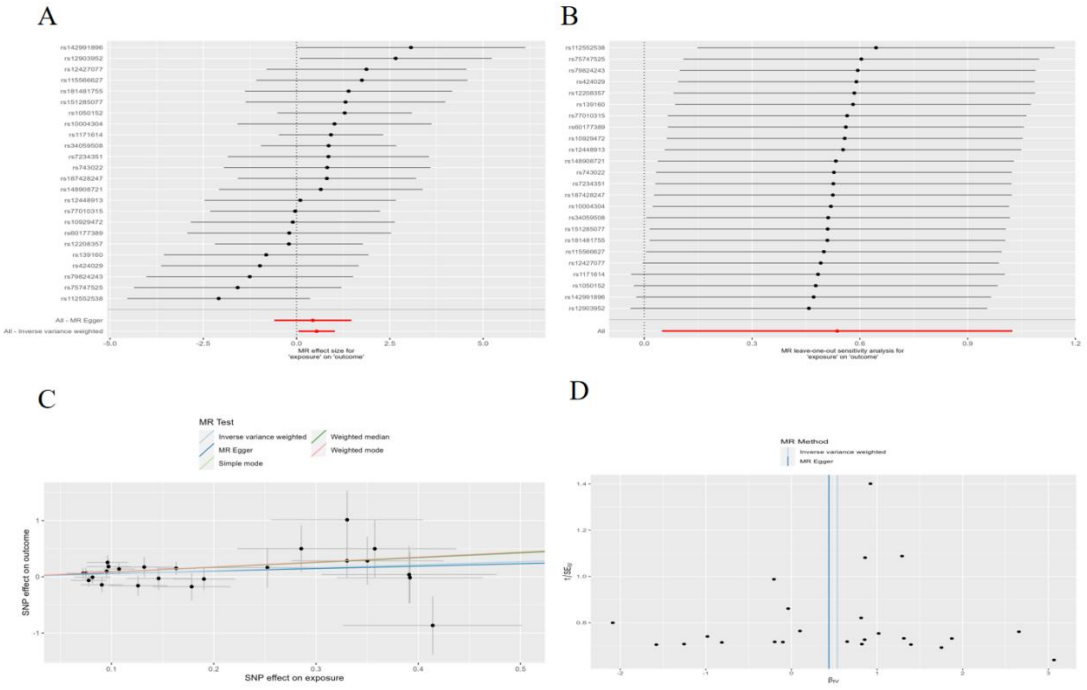

Supplementary Figure 43. Forest plot (A), sensitivity analysis (B), scatter plot (C), and funnel plot (D) of the causal effect of X-24241 levels on PDAC risk.

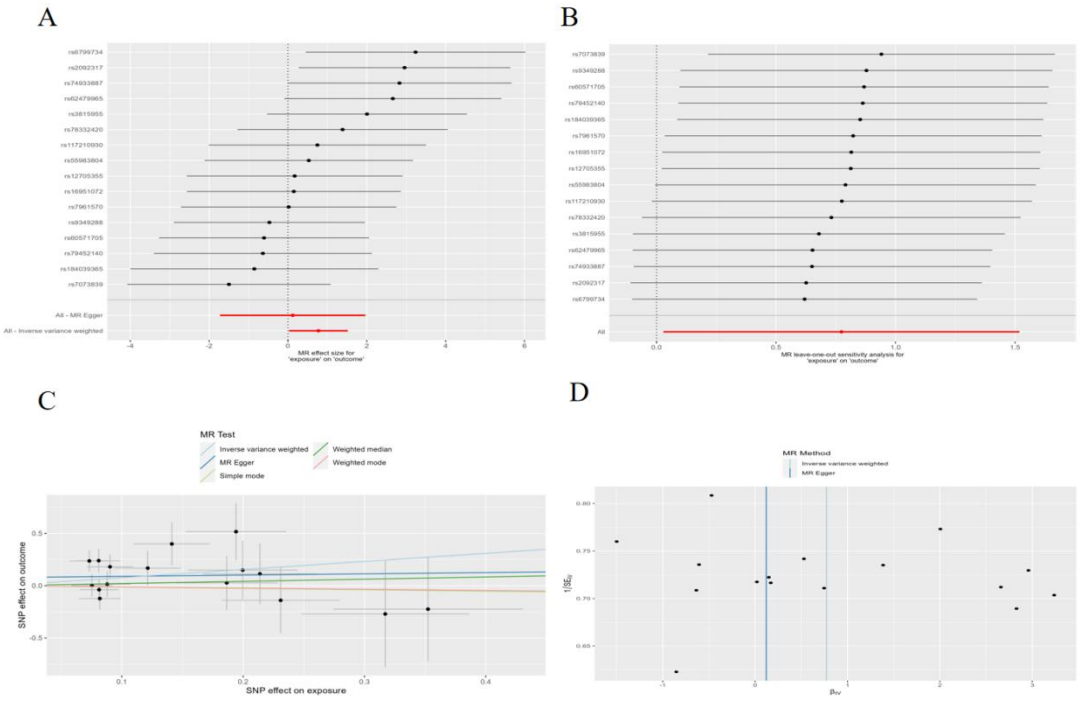

Supplementary Figure 44. Forest plot (A), sensitivity analysis (B), scatter plot (C), and funnel plot (D) of the causal effect of X-25520 levels on PDAC risk.

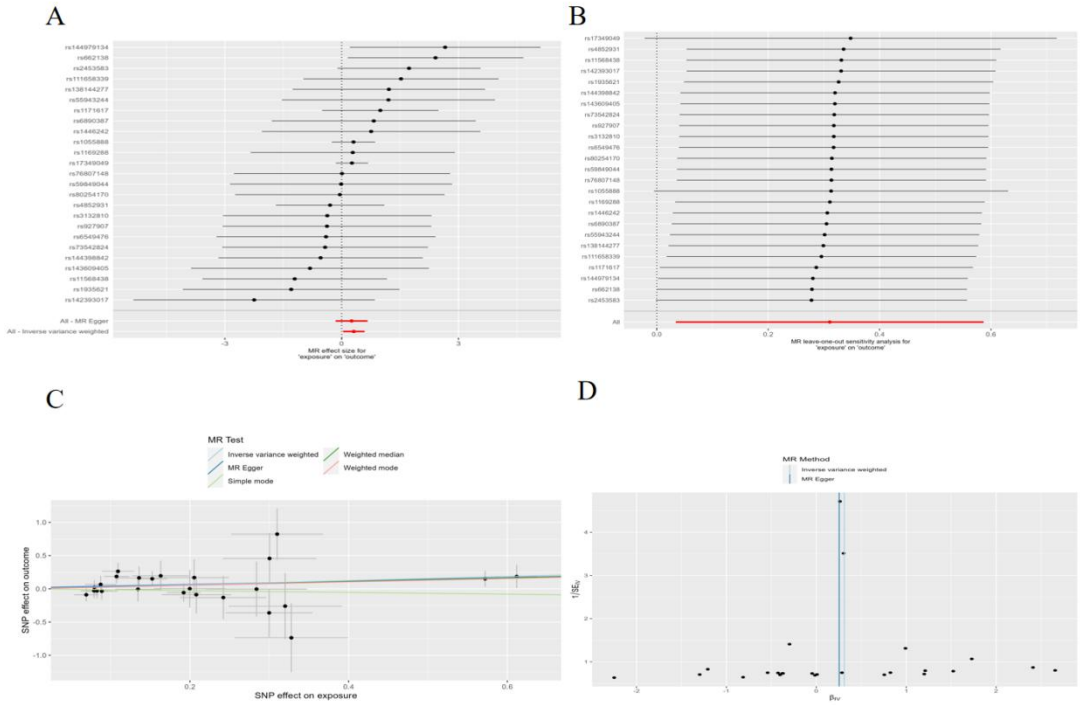

Supplementary Figure 45. Forest plot (A), sensitivity analysis (B), scatter plot (C), and funnel plot (D) of the causal effect of N-acetylarginine levels on PDAC risk.

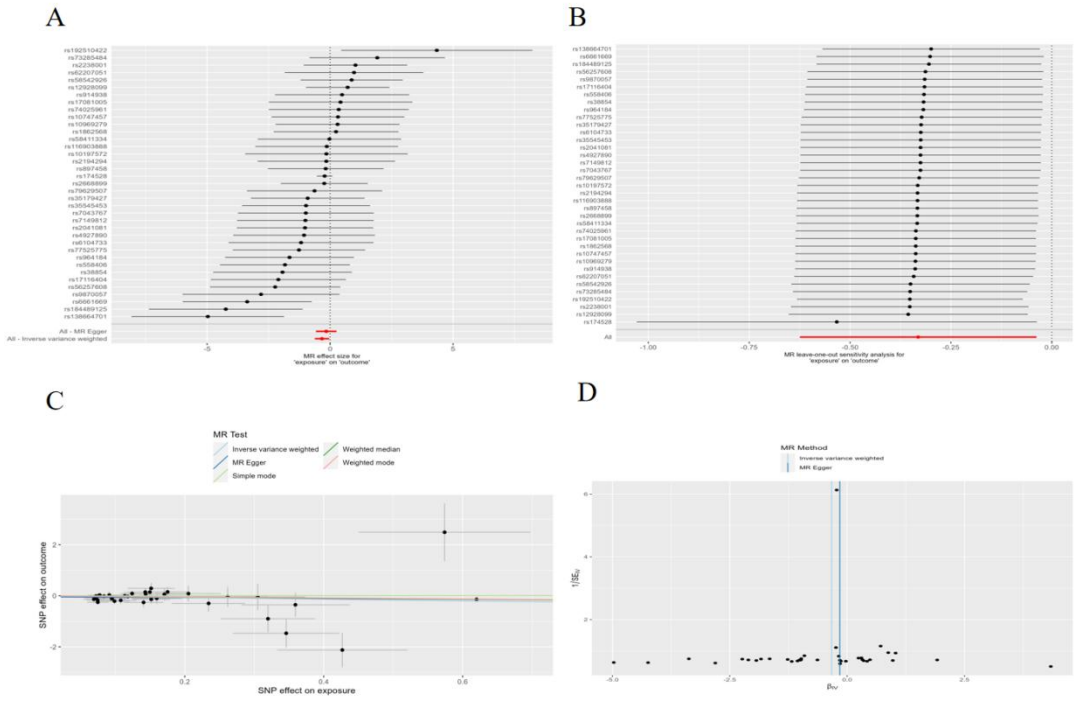

Supplementary Figure 46. Forest plot (A), sensitivity analysis (B), scatter plot (C), and funnel plot (D) of the causal effect of 1-stearoyl-2-arachidonoyl-gpc (18:0/20:4) levels on PDAC risk.

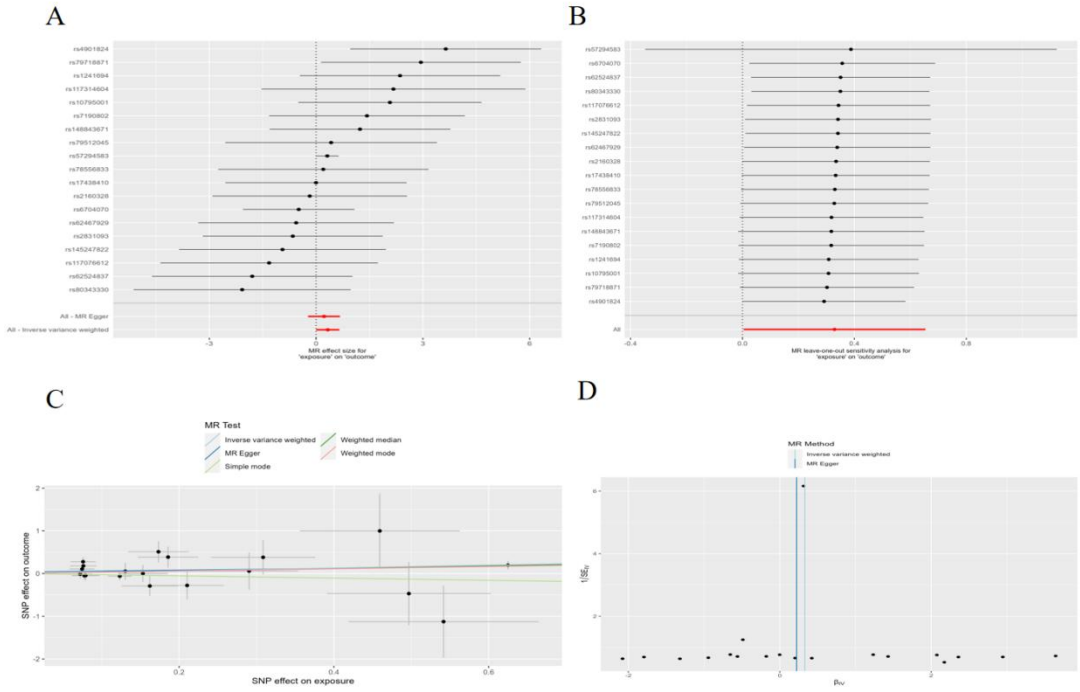

Supplementary Figure 47. Forest plot (A), sensitivity analysis (B), scatter plot (C), and funnel plot (D) of the causal effect of 2'-o-methylcytidine levels on PDAC risk.

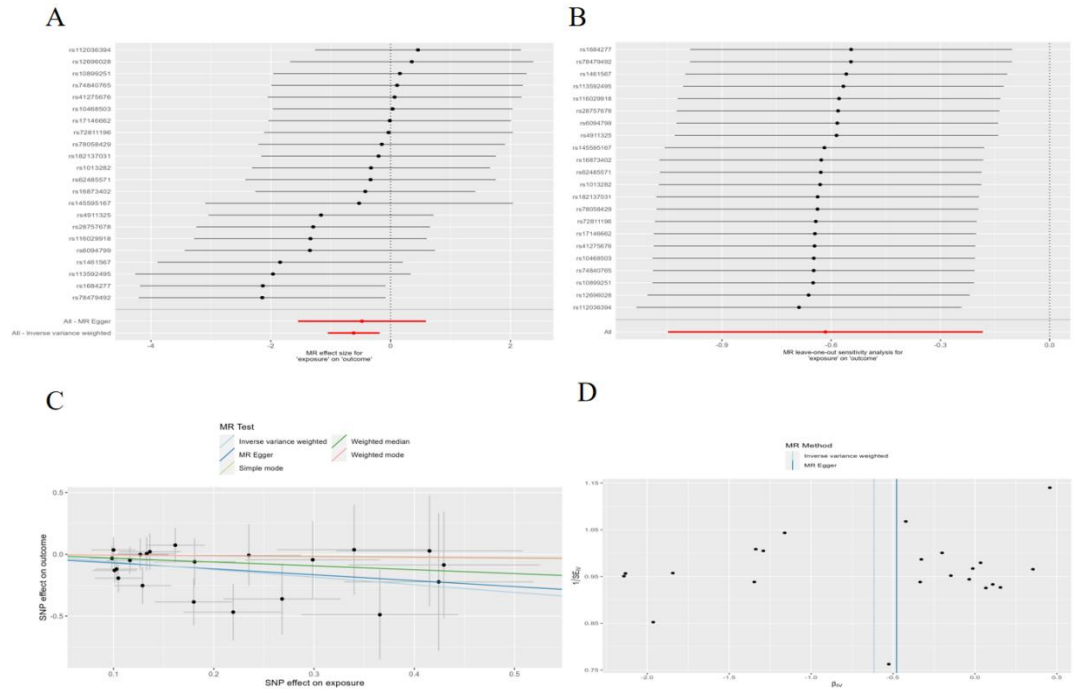

Supplementary Figure 48. Forest plot (A), sensitivity analysis (B), scatter plot (C), and funnel plot (D) of the causal effect of Adenosine 5'-diphosphate (ADP) to phosphoethanolamine ratio on PDAC risk.

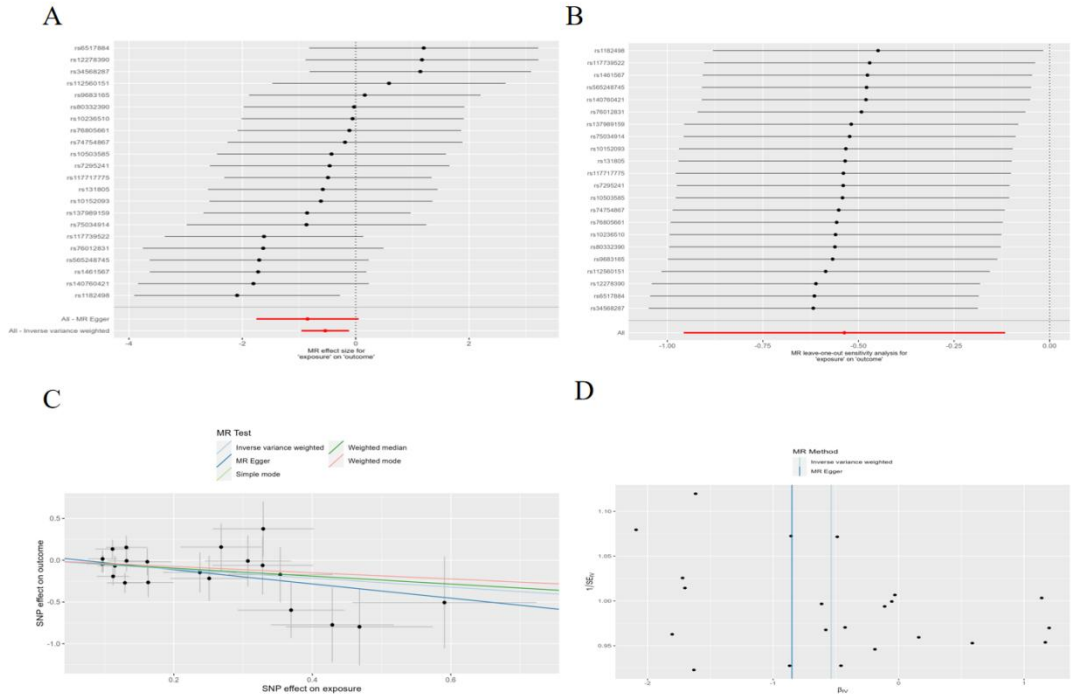

Supplementary Figure 49. Forest plot (A), sensitivity analysis (B), scatter plot (C), and funnel plot (D) of the causal effect of Adenosine 5'-diphosphate (ADP) to 2'-deoxyuridine ratio on PDAC risk.

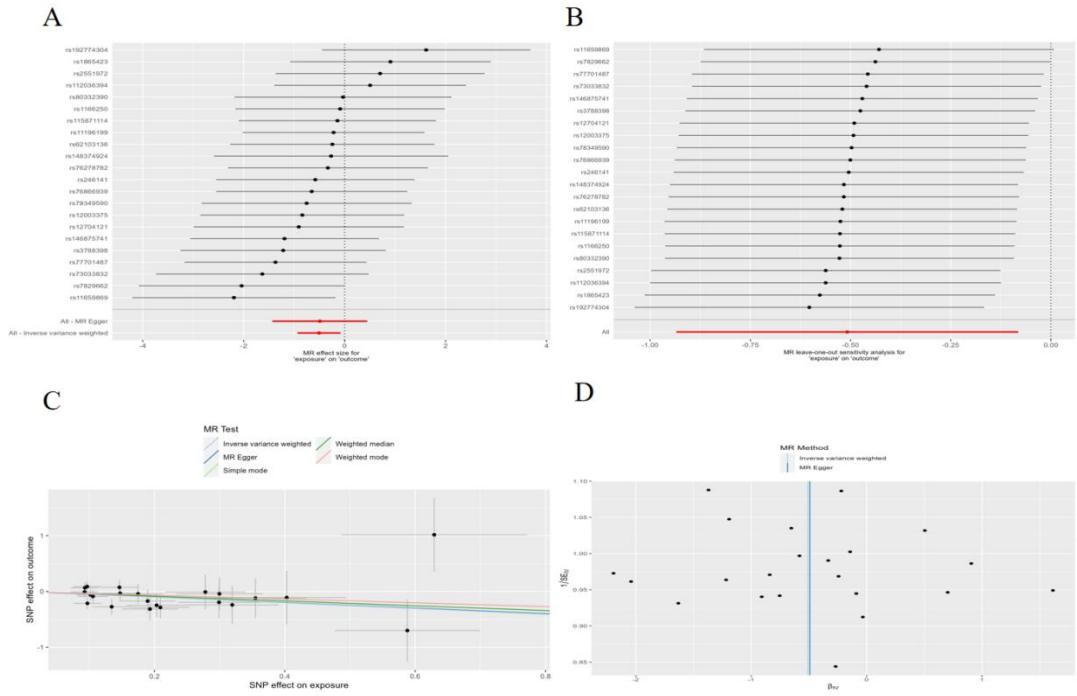

Supplementary Figure 50. Forest plot (A), sensitivity analysis (B), scatter plot (C), and funnel plot (D) of the causal effect of Adenosine 5'-diphosphate (ADP) to gluconate ratio on PDAC risk.

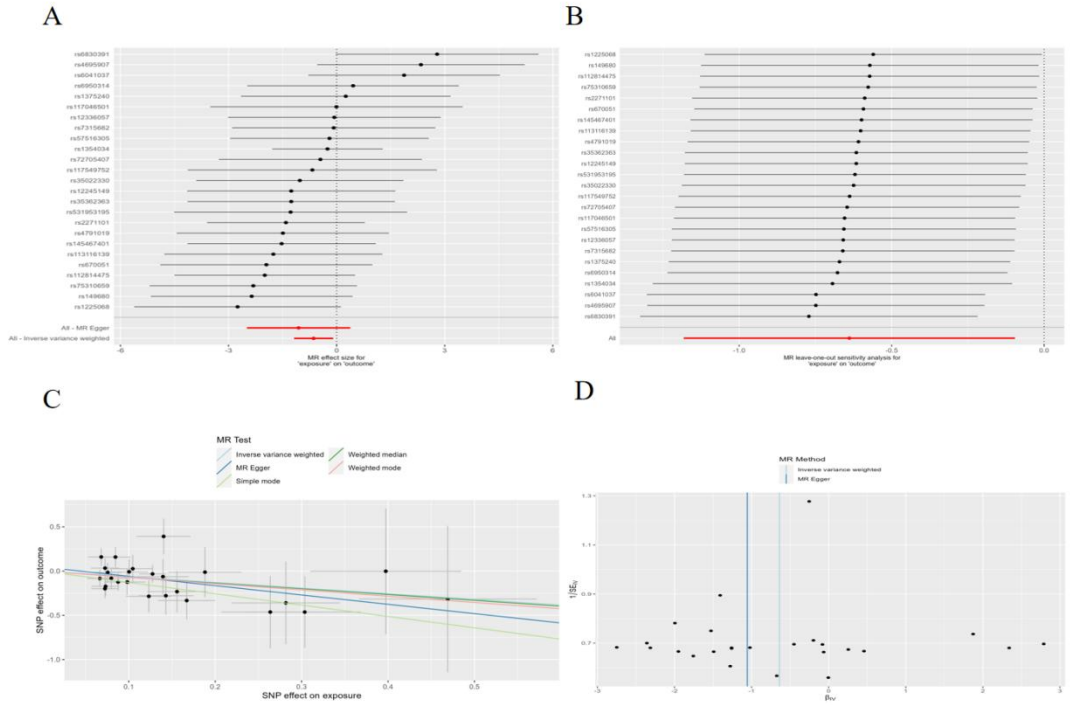

Supplementary Figure 51. Forest plot (A), sensitivity analysis (B), scatter plot (C), and funnel plot (D) of the causal effect of Aspartate to glutamate ratio on PDAC risk.

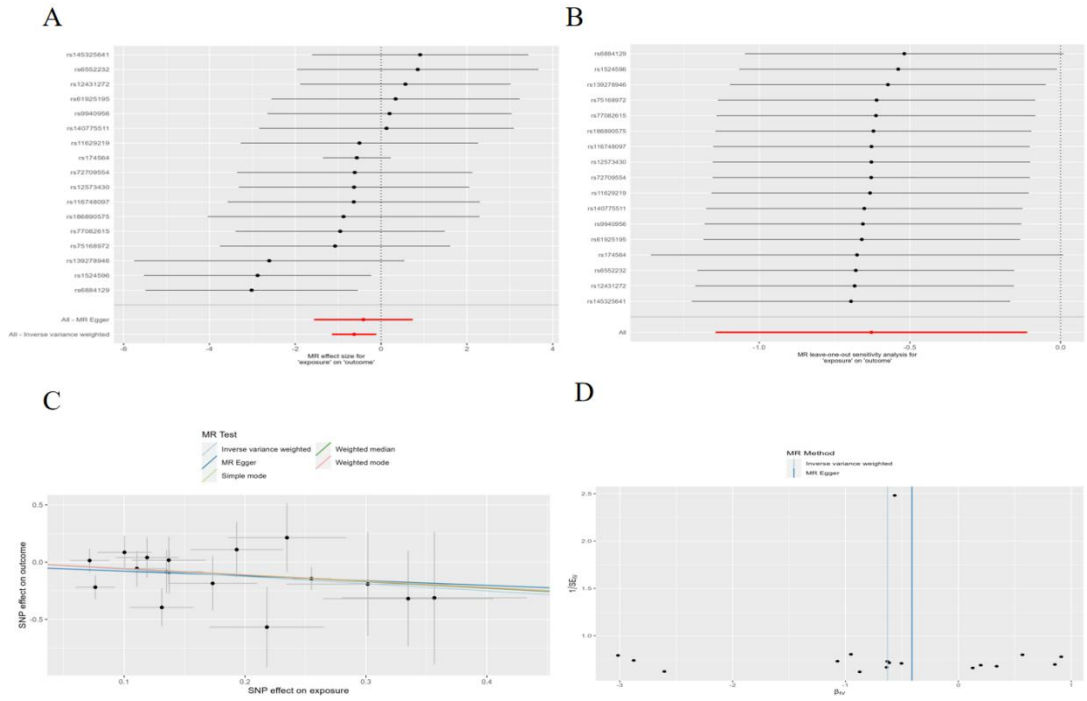

Supplementary Figure 52. Forest plot (A), sensitivity analysis (B), scatter plot (C), and funnel plot (D) of the causal effect of Arachidonate (20:4n6) to pyruvate ratio on PDAC risk.

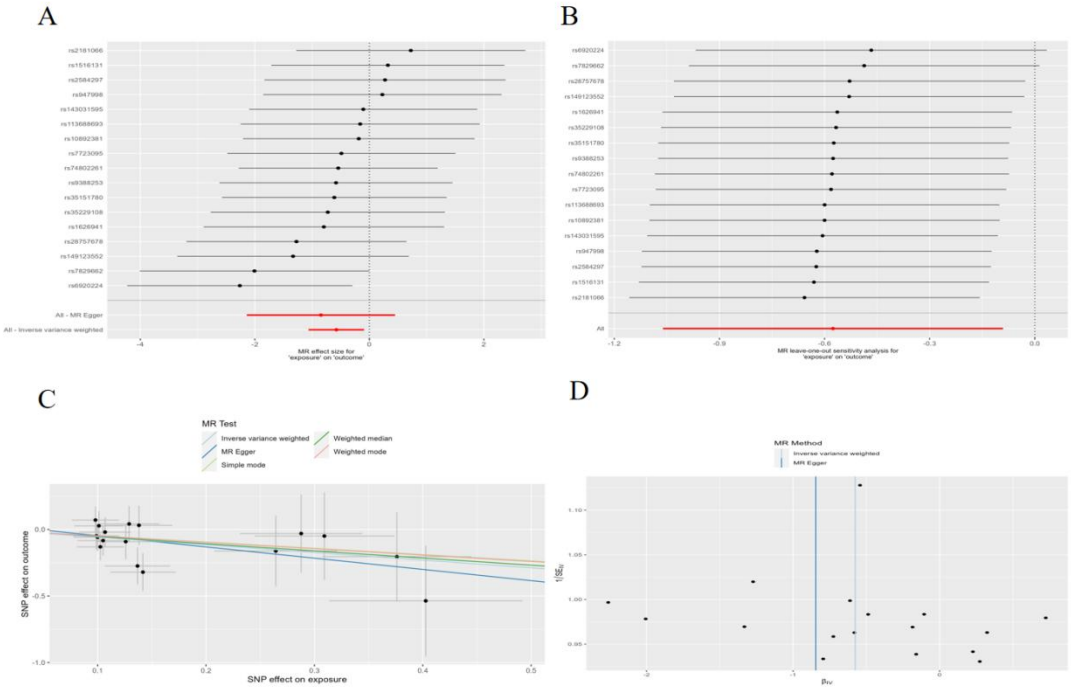

Supplementary Figure 53. Forest plot (A), sensitivity analysis (B), scatter plot (C), and funnel plot (D) of the causal effect of Adenosine 5'-diphosphate (ADP) to glycerate ratio on PDAC risk.

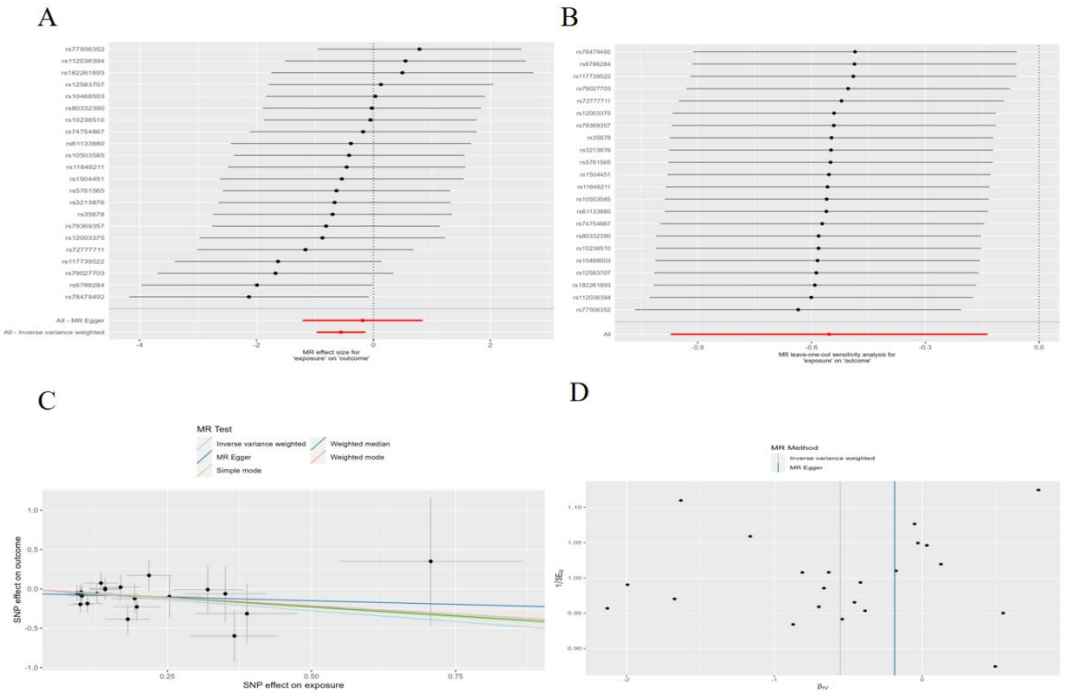

Supplementary Figure 54. Forest plot (A), sensitivity analysis (B), scatter plot (C), and funnel plot (D) of the causal effect of Adenosine 5'-diphosphate (ADP) to valine ratio on PDAC risk.

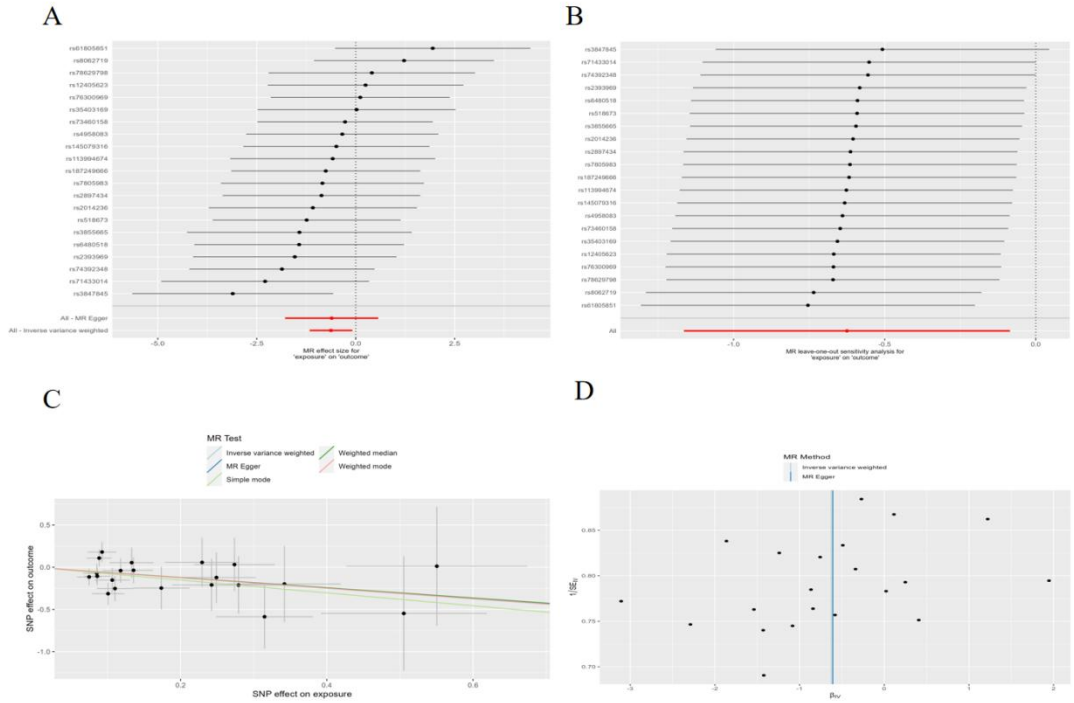

Supplementary Figure 55. Forest plot (A), sensitivity analysis (B), scatter plot (C), and funnel plot (D) of the causal effect of Cortisol to 4-cholesten-3-one ratio on PDAC risk.

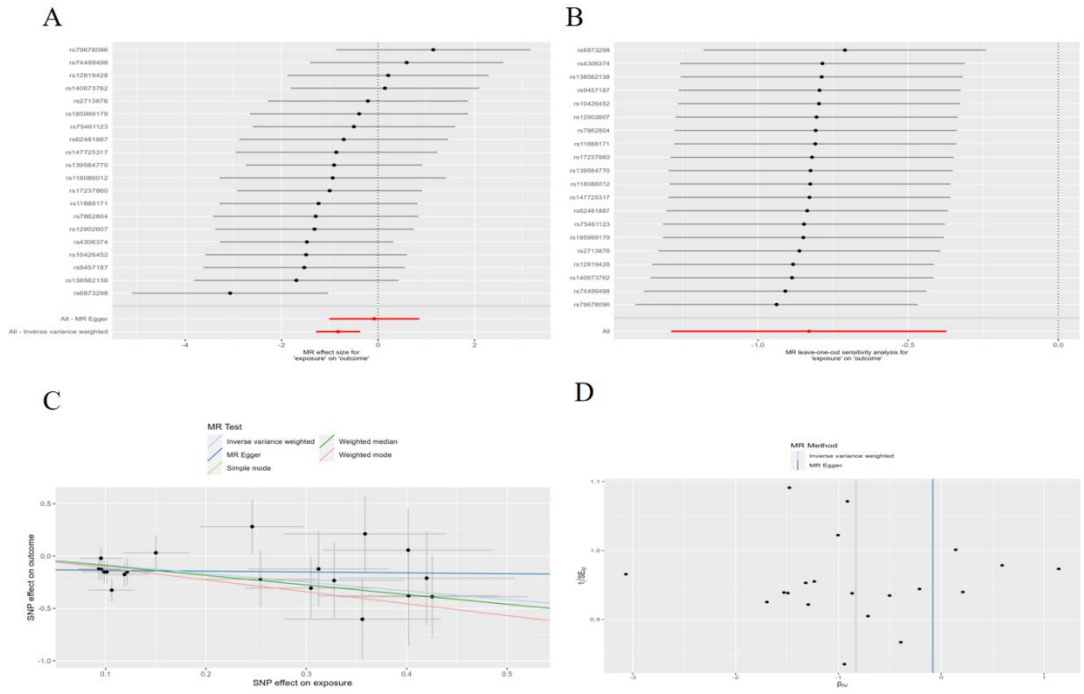

Supplementary Figure 56. Forest plot (A), sensitivity analysis (B), scatter plot (C), and funnel plot (D) of the causal effect of Inosine to theophylline ratio on PDAC risk.

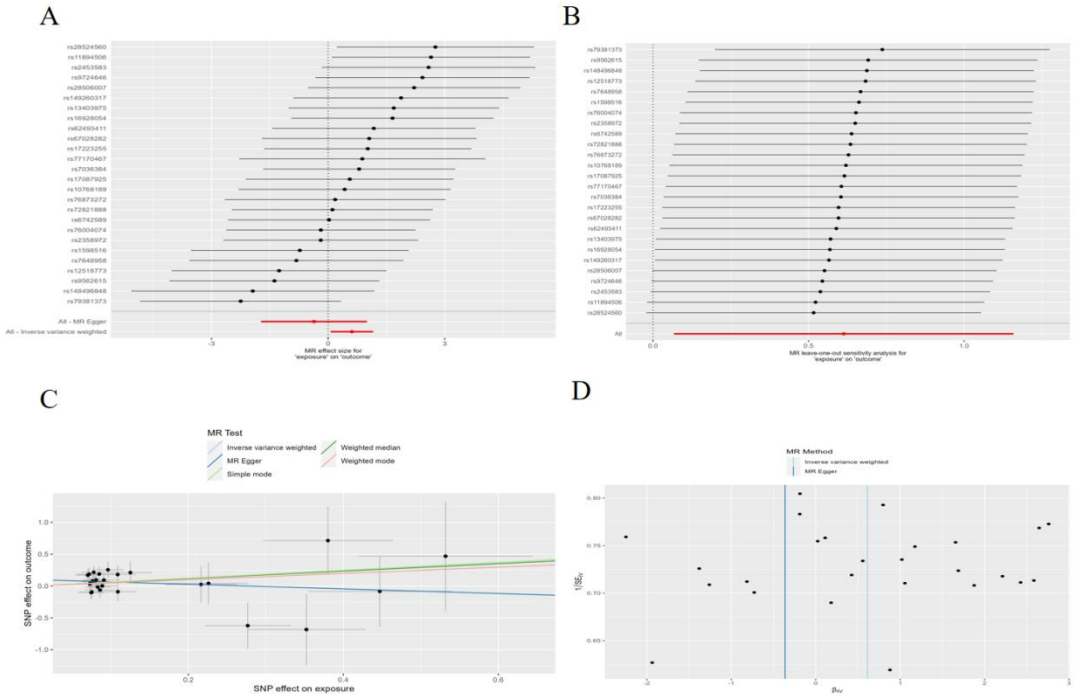

Supplementary Figure 57. Forest plot (A), sensitivity analysis (B), scatter plot (C), and funnel plot (D) of the causal effect of Tryptophan to pyruvate ratio on PDAC risk.

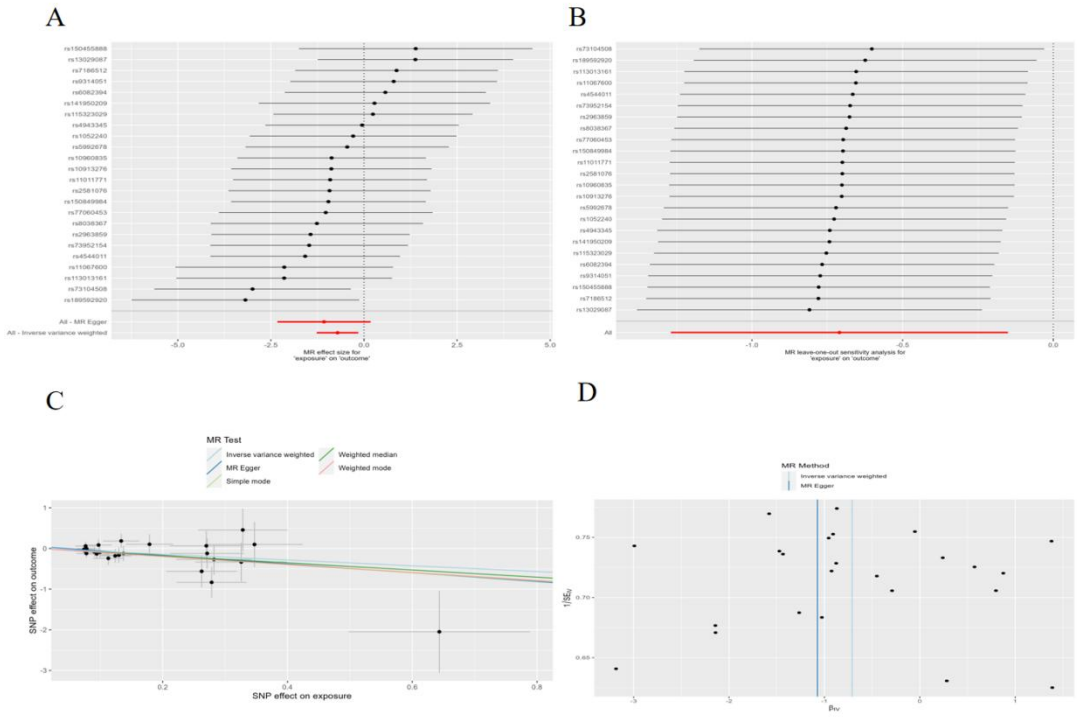

Supplementary Figure 58. Forest plot (A), sensitivity analysis (B), scatter plot (C), and funnel plot (D) of the causal effect of Glycerol to mannitol to sorbitol ratio on PDAC risk.

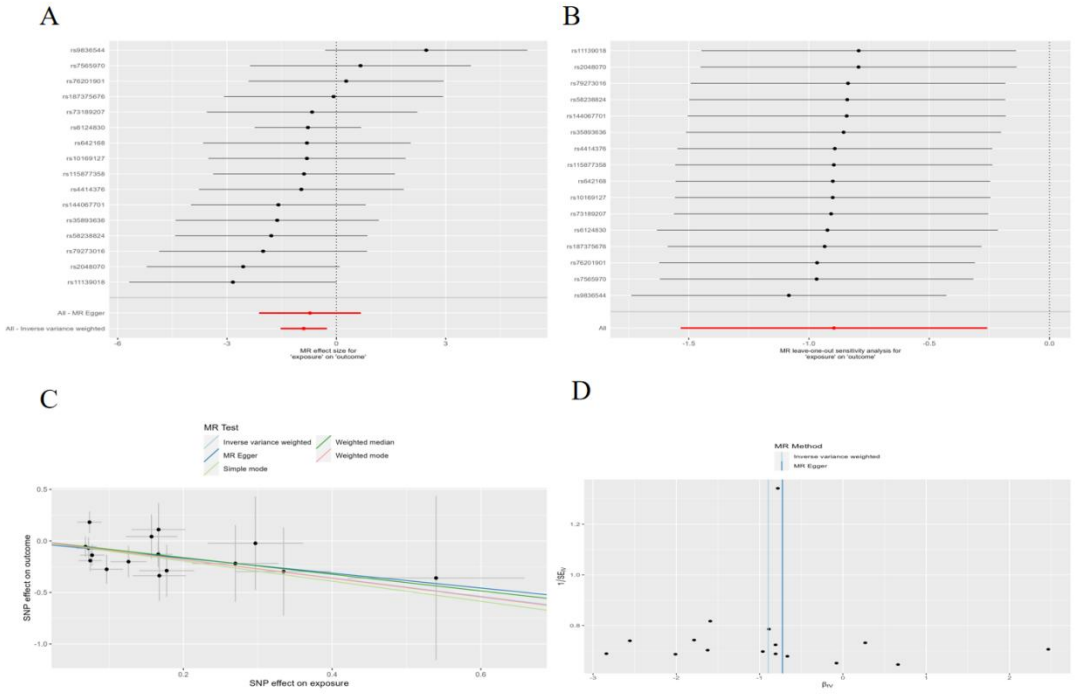

Supplementary Figure 59. Forest plot (A), sensitivity analysis (B), scatter plot (C), and funnel plot (D) of the causal effect of Alpha-ketoglutarate to pyruvate ratio on PDAC risk.

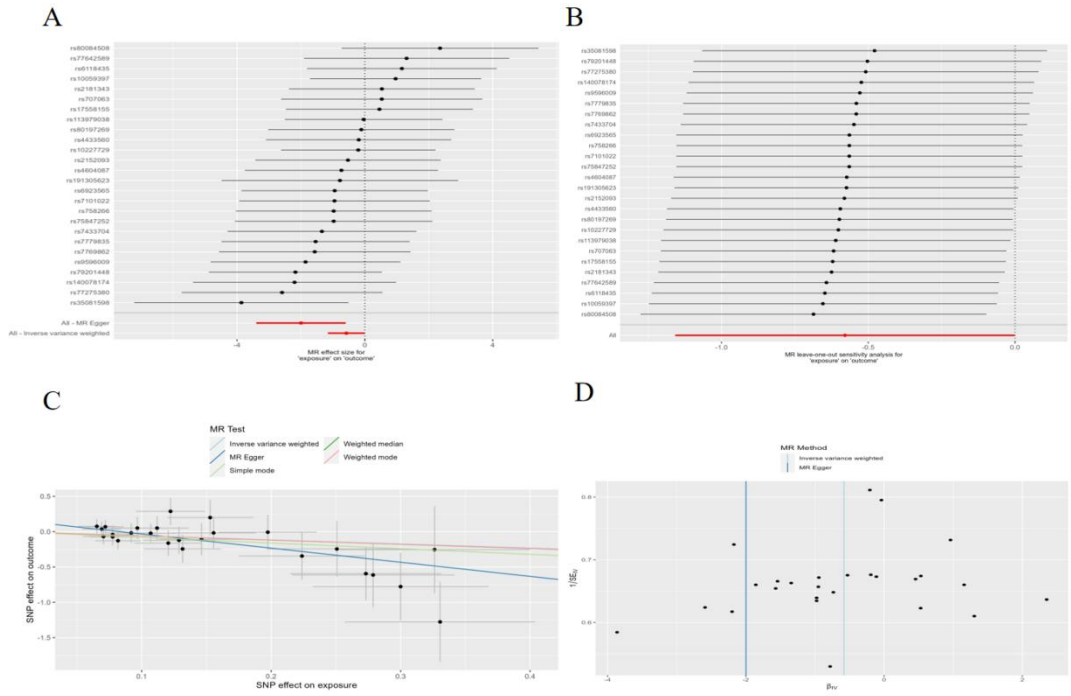

Supplementary Figure 60. Forest plot (A), sensitivity analysis (B), scatter plot (C), and funnel plot (D) of the causal effect of Leucine to phosphate ratio on PDAC risk.

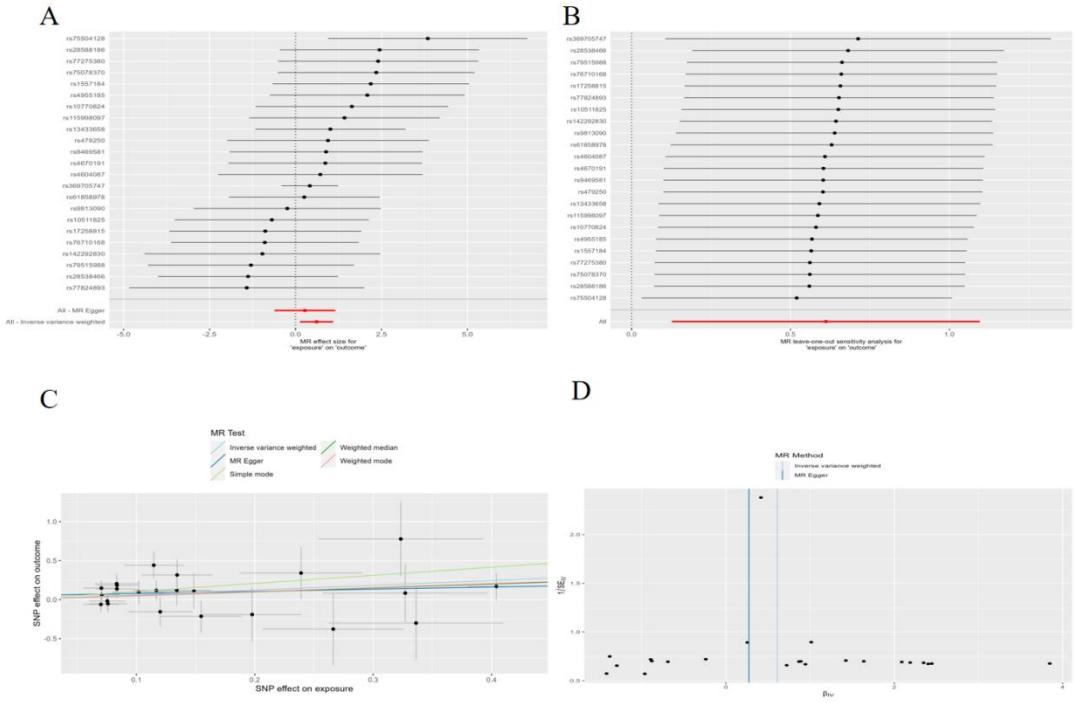

Supplementary Figure 61. Forest plot (A), sensitivity analysis (B), scatter plot (C), and funnel plot (D) of the causal effect of Phosphate to proline ratio on PDAC risk.

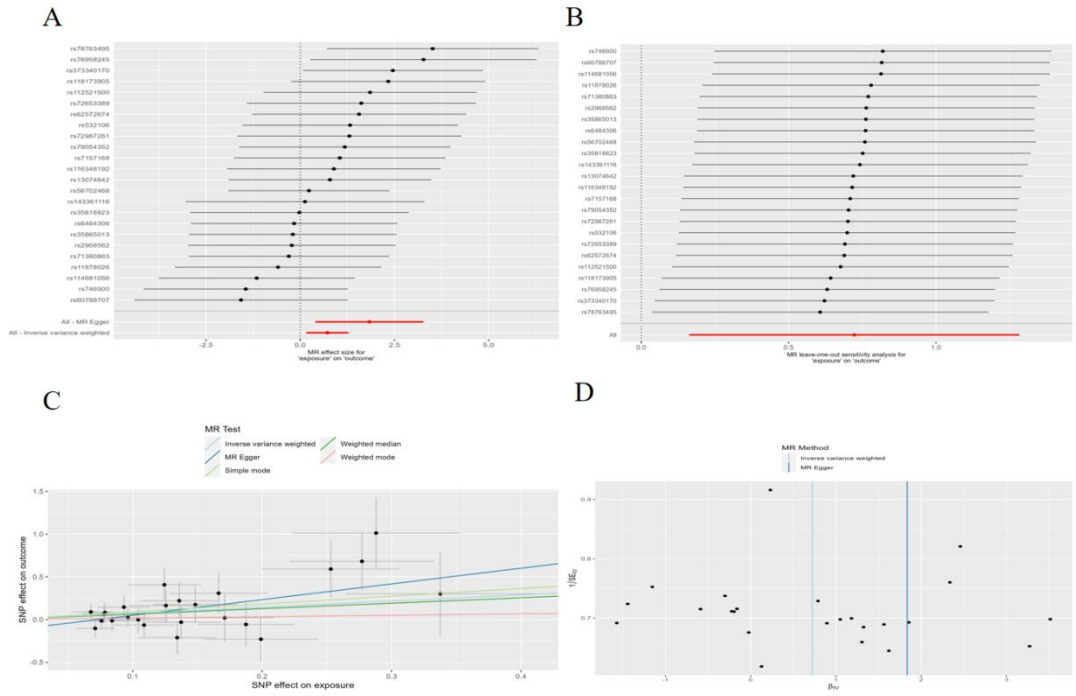

Supplementary Figure 62. Forest plot (A), sensitivity analysis (B), scatter plot (C), and funnel plot (D) of the causal effect of Phosphoethanolamine to choline ratio on PDAC risk.

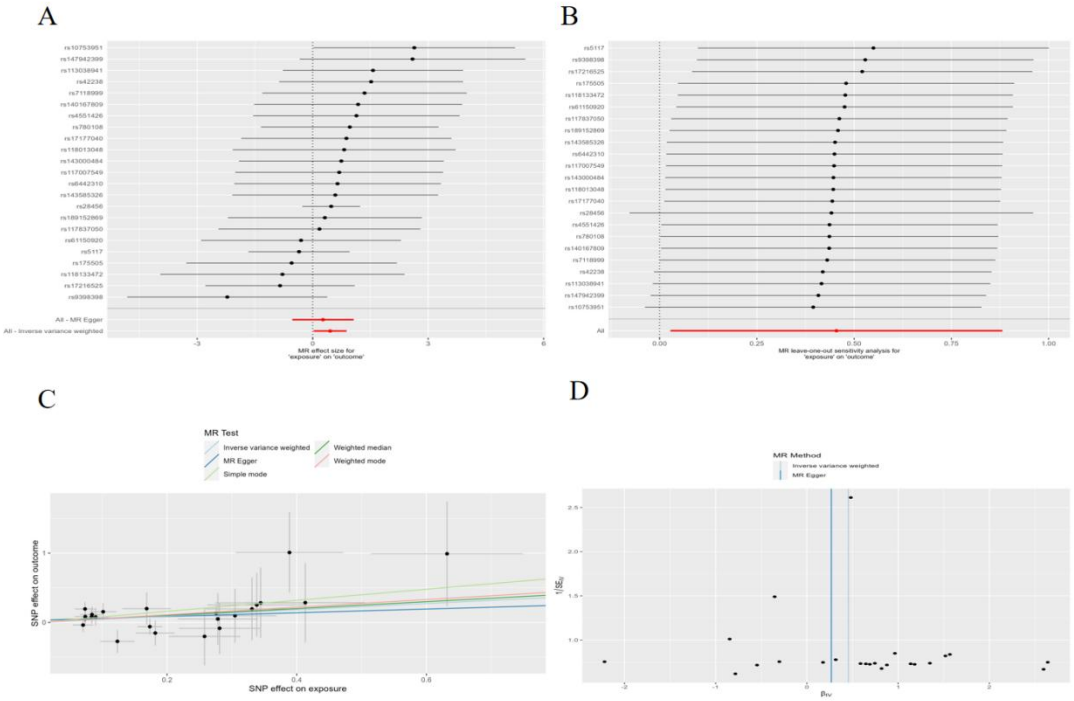

Supplementary Figure 63. Forest plot (A), sensitivity analysis (B), scatter plot (C), and funnel plot (D) of the causal effect of Cholesterol to linoleoyl-arachidonoyl-glycerol (18:2 to 20:4) [1] ratioon PDAC risk.

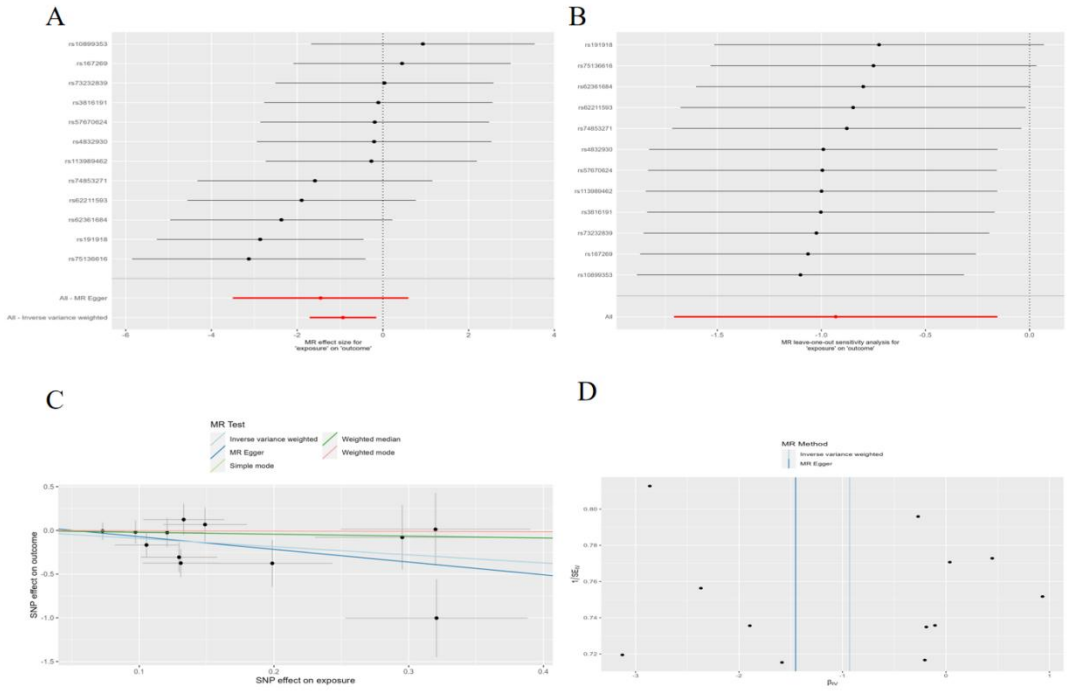

Supplementary Figure 64. Forest plot (A), sensitivity analysis (B), scatter plot (C), and funnel plot (D) of the causal effect of Cholesterol to benzoate ratio PDAC risk.

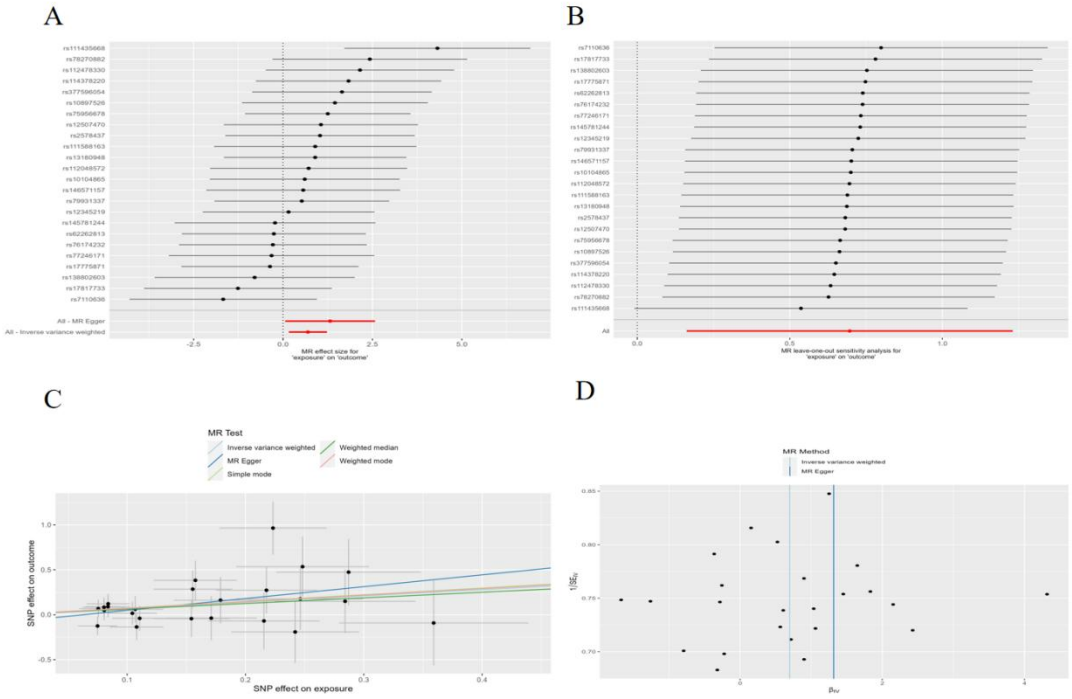

Supplementary Figure 65. Forest plot (A), sensitivity analysis (B), scatter plot (C), and funnel plot (D) of the causal effect of Salicylate to taurocholate ratio PDAC risk.

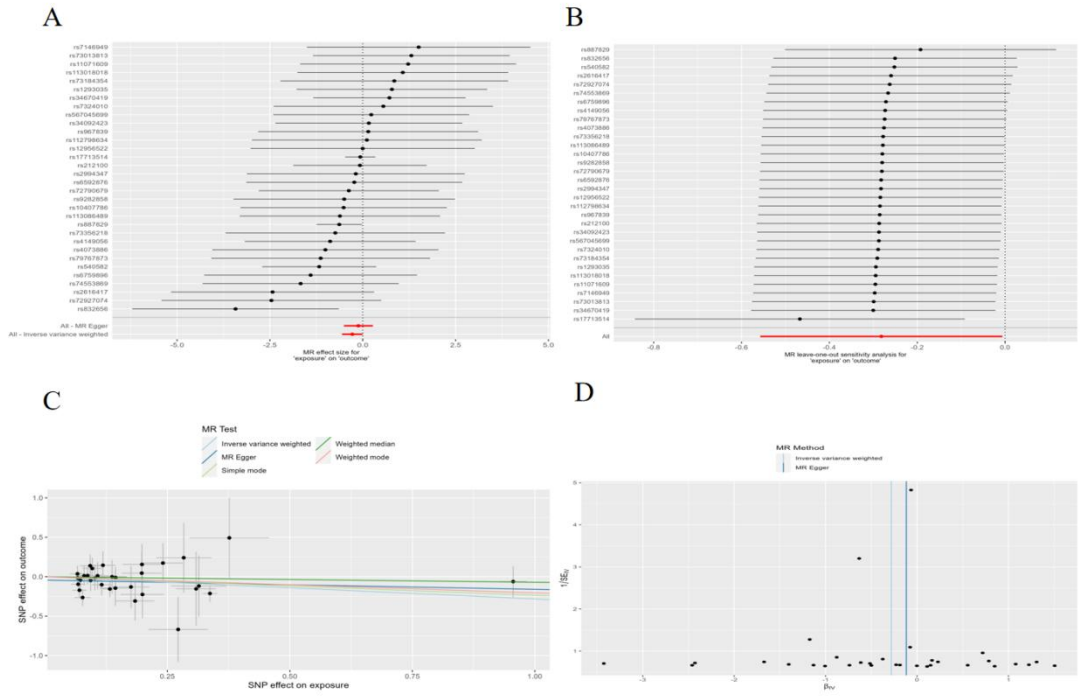

Supplementary Figure 66. Forest plot (A), sensitivity analysis (B), scatter plot (C), and funnel plot (D) of the causal effect of Bilirubin (Z,Z) to androsterone glucuronide ratio PDAC risk.

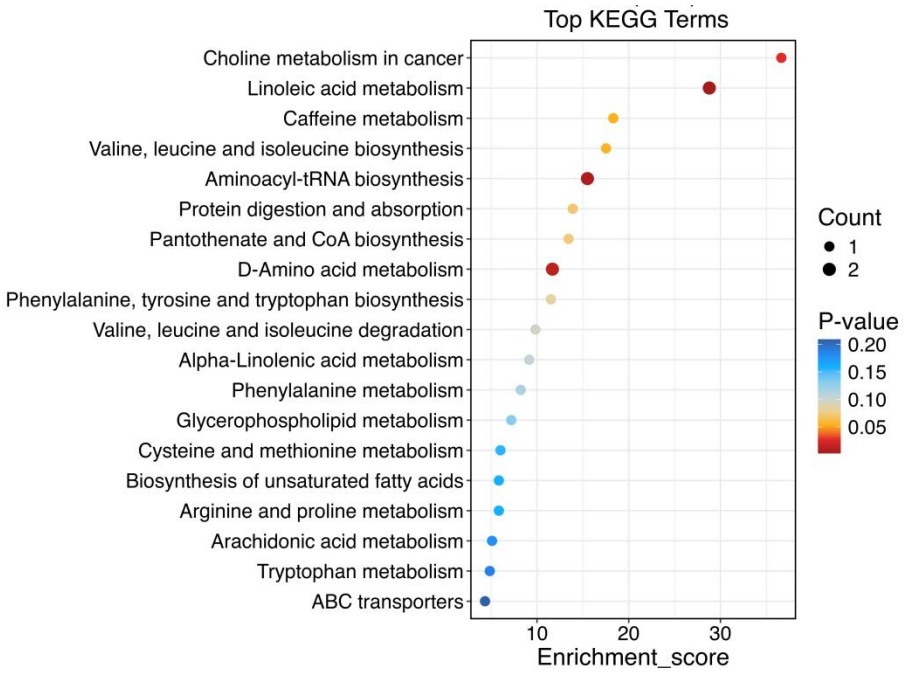

Supplementary Figure 67. KEGG pathway bubble plots of 36 significant metabolites.

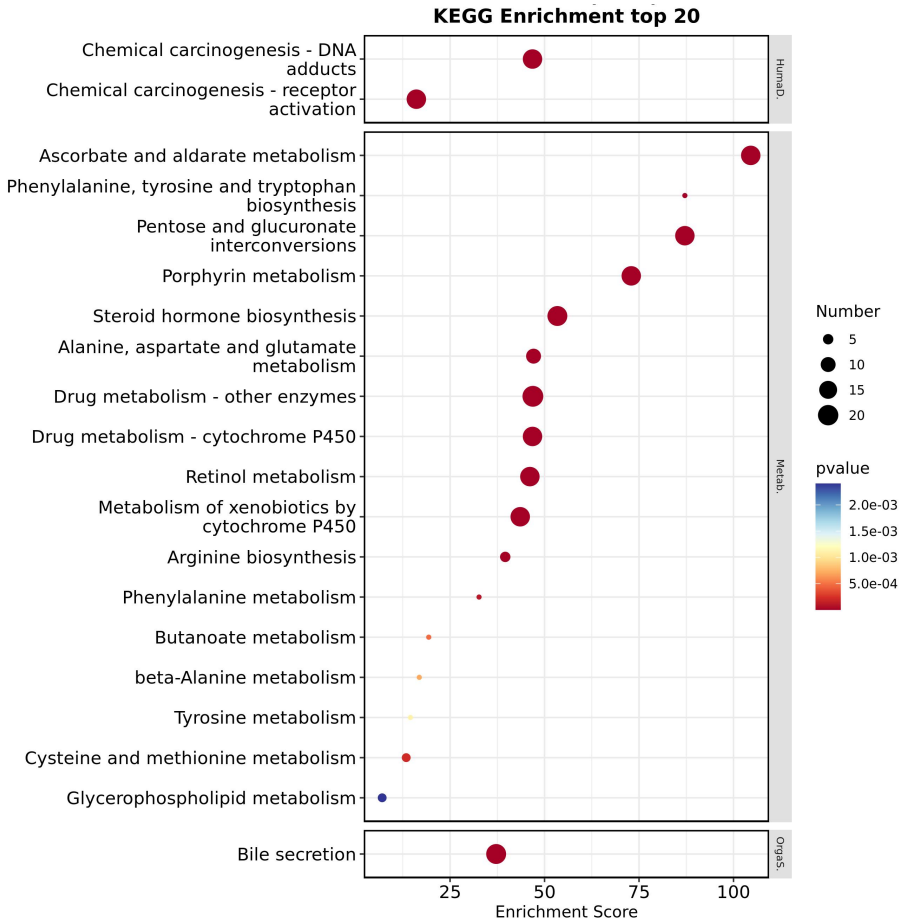

Supplementary Figure 68. Top20 KEGG pathway bubble plots of shared proteins corresponding to 19 significant metabolite ratios.